August 1965

Submitted to

GEORGE C. MARSHALL SPACE FLIGHT CENTER

NATIONAL AERONAUTICS AND SPACE ADMINISTRATION

HUNTSVILLE, ALABAMA

BUREAU OF ENGINEERING RESEARCH

Progress Report No. 5

for

NASA Contract NAS8-11155

COMPARISON OF SEVERAL ANALYTICAL SOLUTIONS TO THE SHEAR LAG PROBLEM WITH EXPERIMENTAL DATA

by

Dennis M. Rigsby

BER

COLLEGE OF ENGINEERING

THE UNIVERSITY OF ALABAMA 1831

UNIVERSITY OF ALABAMA

UNIVERSITY ALABAMA

Progress Report No. 5

for

NASA Contract NAS8-11155

Preliminary Data

COMPARISON OF SEVERAL ANALYTICAL SOLUTIONS TO THE SHEAR LAG PROBLEM WITH EXPERIMENTAL DATA

by

Dennis M. Rigsby

Submitted to

GEORGE C. MARSHALL SPACE FLIGHT CENTER

NATIONAL AERONAUTICS AND SPACE ADMINISTRATION

BUREAU OF ENGINEERING RESEARCH

UNIVERSITY OF ALABAMA

UNIVERSITY, ALABAMA

AUGUST 1965

ACKNOWLEDGEMENT

The author wishes to express his appreciation to his Thesis Committee Chairman, Professor William K. Rey of the Aerospace Engineering Department of the University of Alabama, for his suggestion of this thesis topic and his many helpful suggestions throughout the course of the investigation.

Appreciation is extended to the other members of his thesis committee, Professor Colgan H. Bryan, Professor Raymond M. Hollub and Professor Howard W. King.

TABLE OF CONTENTS

		Page
ACKNOWLEDGEMENT		ii
LIST OF ILLUSTRATIONS		iv
LIST OF SYMBOLS		v
Chapter		
I.	INTRODUCTION	1
II.	COMPARISON OF ANALYTICAL SOLUTIONS WITH EXPERIMENTAL DATA	7
III.	CONCLUSIONS	11
APPENDIX A.	DIFFERENTIAL EQUATION SOLUTION	27
APPENDIX B.	MINIMUM POTENTIAL ENERGY EQUATIONS	36
APPENDIX C.	STRESS FUNCTION SOLUTION	43
APPENDIX D.	SUBSTITUTE SINGLE STRINGER METHOD	67
APPENDIX E.	MINIMUM ENERGY SOLUTION USING MATRIX METHODS	74
LIST OF REFERENCES		77

LIST OF ILLUSTRATIONS

Figure		Page
1	Dimensioned Sketch of Panel B	
2	Dimensioned Sketch of Panel C	
3	Comparison of Differential Equation Type Solution with Experimental Data for Panel B	
4	Comparison of Differential Equation Type Solution with Experimental Data for Panel C	
5	Comparison of Minimum Potential Energy Solution with Experimental Data for Panel B	
6	Comparison of Minimum Potential Energy Solution with Experimental Data for Panel C	
7	Comparison of Stress Function Type Solution with Experimental Data for Panel C	
8	Comparison of Stringer-Sheet Theory with Experimental Data for Panel B	
9	Comparison of Stringer-Sheet Theory with Experimental Data for Panel C	
10	Comparison of Substitute Stringer Solution with Experimental Data for Panel B	
11	Comparison of Substitute Stringer Solution with Experimental Data for Panel C	
12	Comparison of Matrix Method Solution with Experimental Data for Panel B	
13	Comparison of Matrix Method Solution with Experimental Data for Panel C	

TABLE OF SYMBOLS

A	cross sectional area of stiffener, in^2, when used with a subscript. Also used as an arbitrary constant in Appendix C.
A_F	area of flange, in^2
A_L	area of stiffener, in^2
a	one half panel width, in
B	arbitrary constant used in Appendix C
b	distance between stiffeners, in
b_c	distance from centroid of flange to centroid of areas of remaining stiffeners, in
b_s	distance from centroid of flange to centroid of substitute-single stringer, in
c	constant
D	differential operator denoting $\frac{d}{dx}$
e	base of natural logarithms
E	Young's modulus
F	end load used in Appendix B
G	modulus of rigidity
I	unit matrix
k_x	dimensionless parameter used in stress function solution, $k_x = (1 + \frac{tx}{t})$
k_y	dimensionless parameter used in stress function solution, $k_y = (1 + \frac{ty}{t})$
k	parameter used in minimum potential energy equations, Appendix B. $k = \left(\frac{Gt}{bEA_s}\right)^{1/2}$
L	length of panel
M	coefficient matrix used in differential equation solution, Appendix A

m	$\frac{A_F}{A_L}$ in minimum potential energy solution,
	$\frac{A_F}{ak_x t}$ in stress function solution
n	number of stringers in half panel or when used as a subscript it represents the number of the stiffener or panel under consideration
O	origin of cartesian coordinate system
P	applied axial load, pounds
P_o	uniform stress of infinity, psi
P_x	average normal stress in direction O_x, psi
P_y	average normal stress in direction O_y, psi
q	shear flow, lb/in
s	circumferential distance
t	thickness of sheet material
t_x	area of reinforcing material added in direction O_x, per unit width of sheet
t_y	area of reinforcing material added in direction O_y, per unit width of sheet
T_o	end load, stress function solution, pounds
T_∞	load at infinity, pounds
U	strain energy
α	variable used in stress function solution
β	angle of rotation, stringer-sheet solution
γ	shearing strain
ε	normal strain
ζ	$\frac{\lambda}{0.04712}$
θ_n	roots to transcendental equation, stress function solution and stringer sheet solution

λ	parameter used in differential equation solution
μ	Poisson's ratio
π	ratio of circumference of circle to diameter, approximately 3.1416
σ	normal stress
τ	shearing stress
Φ	stress function
φ	variable used in minimum potential energy solution

CHAPTER I

STATEMENT OF THE PROBLEM

Shear lag is the term commonly used to describe the influence that shearing deformations have on the stress distribution in sheet-stringer types of construction [2][1]. Experimental evidence has shown that the stress distribution in sheet-stringer structures subjected to bending cannot be adequately predicted by the elementary flexure theory. The difference between the stress distribution predicted by elementary flexure theory and the experimentally determined distribution is due in part to the fact that the theoretical assumption that plane sections remain plane after bending is not satisfied in sheet-stringer structures. If plane sections remained plane after bending, the sheet between stringers would have to have infinite shearing rigidity, i.e., no shearing strains. Since the thin sheet between stiffeners actually has very little shear stiffness and the sheet suffers large shearing deformations under load, the assumption of infinite shearing rigidity is not satisfied in this type of structure. As a result of these shear deformations, the stresses in the stringers are less than the predicted stresses. Since the stringer stresses lag behind predicted values, the effect has been described as shear lag.

Thus, the problem of the stress analyst is the determination of the stress distribution in box beams taking into consideration shearing strains. In a hollow, rectangular box beam under pure bending, the surface under compression behaves as a flat, stiffened panel subjected to an axial compressive load. In this thesis a flat stiffened panel under axial load has been investigated.

---

[1]Numbers in brackets refer to references listed in the bibliography.

Survey of Previous Work

Although many investigators have obtained solutions to the shear lag problem, all of their solutions appear to have shortcomings. Because of the simplifying assumptions made, some of the less rigorous solutions are valid only for certain special cases, while some of the more mathematically rigorous solutions are quite cumbersome to apply.

One of the first investigators in the United States to give much attention to the problem was Younger in 1930 [30]. He presented formulas for the efficiency of a box beam with walls of uniform thickness, which may be considered as the limiting case of a large number of very small stringers. His analysis is limited by the assumption of a constant cross section.

Many investigators attempted to solve the problem by first deriving the differential equations of equilibrium of either the stringers or the sheet material and then solving the equations for the stresses by one of several methods. Winny [29], one of the early British investigators, obtained a Fourier series solution to the differential equations of equilibrium of the stresses in the skin between the spars of a stressed skin wing. Kuhn [20] proposed a numerical integration type solution for the differential equations. Goodey [13] solved the differential equations of equilibrium of the stringer forces using the minimum potential energy theory and the calculus of variations.

In 1946 Goodey [13] published a comprehensive series of articles each concerned with some aspect of the problem of shear lag, or stress diffusion, as it is known to the British. His method of approach required the determination of a stress function for the particular system under consideration. The stress functions he obtained led to expressions

for the stresses which are difficult to use; however, his expressions based on the minimum potential energy theory, mentioned earlier, are very easy to apply.

Borsari and Yu [3] conducted theoretical and experimental investigations of the distribution of strains in a plywood sheet-stringer combination used as the chord member of a box beam acted upon by bending loads. The theoretical solution was obtained with the help of the principle of minimum potential energy and certain simplifying assumptions. Strain measurements were made on a built-up box beam by means of electrical resistance strain gages. A satisfactory agreement between the theoretical and experimental strains was reported.

Fine [10] developed a stress function for the spanwise stress in the flat surface of a box beam under uniformly distributed transverse load. He compared the stresses obtained from this solution with those predicted by the stringer-sheet solution. The two solutions were in good agreement.

Paul Kuhn [19] proposed a solution based upon the use of a substitute single stringer in place of the actual stringers. It was necessary to use a successive approximation method for locating the substitute single stringer. In view of the approximate nature of the solution, Kuhn considered the successive approximations an unwarranted complication. For this reason he developed an empirical one-step method to locate the substitute single stringer [20]. For the empirical determination of the location of the substitute single stringer, shear strain measurements alongside the flanges of three panels of constant section and two panels of variable section were used. Two panels with tapered flanges and a small number of stringers were also investigated. An empirical factor

was chosen based upon the comparison of these tests with theoretical strains predicted by the substitute stringer method. The resulting solution permitted the analysis of multistringer panels with very little computational effort. Results of this type of analysis were good and the method found wide acceptance in industry.

Akao [1] proposed a stress analysis of a rib-stiffened plate based upon the use of groups of orthogonal statically indeterminate force functions. These eigenfunction groups are presented as finite difference equations.

Several investigators have made experimental studies of shear lag. White and Antz [28] reported an investigation made of the stress distribution in thin reinforced panels. Test specimens were constructed of Alclad aluminum sheet reinforced with extruded bulb angles. Results were compared with strains predicted by theory based on the differential equations of equilibrium of the axial forces in the stiffeners. Agreement between experiment and theory indicated the method was well founded.

Lovett and Rodee [21] conducted an experimental investigation of two beams composed of I-sections connected by a stiffened sheet subjected to a uniform bending moment. The result of the investigation was the determination of an effective shear modulus for the sheet in the sheet-stringer combination. It was found that the modulus decreases rapidly under light loadings from the elastic value to some other value depending upon the sheet thickness. The thick sheet gave higher values of effective shear modulus than the thin sheet.

Chiarito [5] reported the results of tests made on two aluminum alloy box beams with corrugated covers. Angles formed from sheet were used for corner flanges in one beam while extruded angles were used for the

corner flanges in the other beam. Electric strain gages were used to measure strains in each beam. The experimental results compared favorably with theoretical results obtained by the substitute-single-stringer theory.

Chiarito [6] also reported the results of an experimental investigation of two box beams loaded to destruction in an effort to verify the shear lag theory at stresses beyond the yield point. An open box beam made of 24S-T aluminum alloy and steel bulkheads was used for the tests. The theoretical and experimental stresses were in good agreement.

Peterson [24] reported the results of tests which were made on a beam having more camber than is likely to be found in an actual wing in order to determine whether the substitute-single-stringer theory might be applied over the entire practical range of camber. Results indicated that the elementary theory overestimates the maximum stress and the substitute-single-stringer theory underestimates it.

In addition to the purely theoretical and experimental solutions already mentioned, some effort has been directed towards an analog type solution. Newton [23] in 1945 and Ross [27] in 1947 proposed a solution based upon the analogy between the distribution of stresses in flat stiffened panels and the distribution of electric current in a ladder type resistance network. The application of this method is limited because the panel must be divided into a finite number of bays having constant stresses. Results of this method were reported to have good agreement with experimental data.

Goland [12] established an analogy between the stress flow in flat stringer-sheet panels and the plane potential flow in an incompressible fluid. The author did not give numerical examples or experimental verification of the method.

The use of a mechanical analogy was proposed by Kuhn [16]. Here, again, the division of the panel into a finite number of bays limits the method.

In the investigation of the bending vibrations of box beams, it is first necessary to determine the shape of the deformed beam due to a static loading. If the effect of shearing deformations are ignored and the elementary theory is used to predict the mode shapes, the predicted natural frequencies can be greatly in error from the actual frequencies. Davenport and Kruszewski [8] found that by using the substitute-single-stringer method in calculating the static stresses and deformations of the beam, the resulting calculated natural frequencies and mode shapes were in much better agreement with experiment.

Purpose and Scope

The objectives of this study were: (1) to consider several of the existing analytical solutions to the shear lag problem, (2) to apply these solutions to a panel with particular properties and loading conditions, (3) to solve for the stress distribution in the panel, and (4) to compare the results of the various theories with experimental data for the same panel with the main objective being the determination of the best method of shear lag analysis.

The following theoretical solutions are treated in the appendices:

Appendix A - Differential equation solution.

Appendix B - Minimum potential energy equations.

Appendix C - Stress function solution.

Appendix D - Substitute-single-stringer method.

Appendix E - Minimum energy solution using matrix methods.

CHAPTER II

COMPARISON OF ANALYTICAL SOLUTIONS WITH EXPERIMENTAL DATA

Experimental Data

The experimental data used in this paper was acquired as part of the performance of National Aeronautics and Space Administration contract No. NAS8-11155 administered by the Bureau of Engineering Research of the University of Alabama under the technical supervision of the George C. Marshall Space Flight Center. Panels B and C referred to in this paper correspond to test panels B and C of the research project referred to above. Details of the experimental procedure, data reduction, and construction of the test panels may be found in Progress Report No. 4 of this contract.

Differential Equation Solution

The differential equations of equilibrium of the normal stresses in the stringers of a stringer-sheet combination are derived in Appendix A of this paper, and one method of solving these equations is presented as a numerical example. The solutions are presented as a linear combination of exponential functions. Results of this solution are compared with experimental data in Figures 3 and 4 for panels B and C, respectively. Examination of Figures 3 and 4 reveals the following information:

1. The theoretical curves and the experimental values for the normal stresses in the stringers indicate the same type stress distribution within the panel. For the loaded stringer, both methods indicate a stress equal to P/A at the loaded end with the value decreasing exponentially as the distance from the

loaded end increases. For the stringer adjacent to the loaded stringer, theory and experiment both indicate normal stresses which increase from zero at the loaded end to a maximum stress then slowly decrease as the distance from the loaded end increases. For the remaining two stringers, theory predicts stresses which increase from zero at the loaded end to some higher value then decrease slowly as the distance from the loaded end increases. The experimental values increase from zero at the loaded end, but do not reach some maximum value then decrease as did the theoretically predicted stresses.

2. Agreement between theory and experiment is poor except at the loaded end. The theoretically predicted stresses for stringers 1, 2, and 3 are non-conservative. For stringer 4 of panel C the predicted stresses are conservative up to a point about 7 inches from the loaded end then they, too, become non-conservative. In panel B the predicted stresses in stringer 4 are conservative up to a point about 15 inches from the loaded end.
3. Overall agreement between theory and experiment is better for panel B than for panel C.

Minimum Potential Energy Equations

Goodey's analysis [11] of the diffusion of end load into a panel having (2N-1) stringers is presented in Appendix B. His final equations have the form of a finite sum of terms involving trigonometric and exponential functions. An analysis of the diffusion of a 2000 pound end load in panels B and C was made using these equations. Results of this analysis are presented in Figures 5 and 6 along with experimental data for comparison. Examination of Figures 5 and 6 reveal the following information:

1. Both experimental and theoretical results indicate that, at some distance from the loaded end, the end load is uniformly distributed among the stringers.
2. For the loaded stringer, the agreement between theory and experiment is good with the best agreement at the loaded end. For panel B, the agreement between theoretically and experimentally predicted stresses is poor except at the loaded end. Agreement between theory and experiment for the unloaded stringers in panel C is fair.
3. Theoretically predicted stresses are conservative.

The Substitute Single Stringer Method

The method for analyzing multistringer panels using a substitute stringer is presented in Appendix D. Results of this method applied to panels B and C having a 2000 pound end load are presented in Figures 10 and 11 with experimental data. Due to the nature of the solution, stresses in the unloaded stringers cannot be predicted; however, it can be seen from the curves that the stresses in the substitute stringer are quite close to the stresses in the stringer adjacent to the loaded stringer. Agreement between predicted stresses and experimental stresses in the loaded stringer is also good.

Minimum Energy Solution Using Matrix Methods

An outline of the analysis of panels B and C utilizing matrix methods based upon the Maxwell-Mohr method is presented in Appendix E. A detailed analysis of this type would be practically impossible without the aid of a digital computer. The Univac 1107, located at the University of Alabama Research Institute, Huntsville, Alabama, was used. Results of these

analyses are presented in Figures 12 and 13 with experimental data. This analysis was performed as part of the National Aeronautics and Space Administration contract previously mentioned, not by the author.

For panel B, the agreement between theory and experiment is fair, better agreement existing in stringer 4 than in the others. The theory is conservative throughout most of the panel. Better overall agreement between theory and experiment exist in the case of panel C, but in this case stringer 4 does not exhibit as good agreement as in panel B. Also, theoretical stresses in stringer 4 were on the non-conservative side.

Stress Function Solution

A stress function for a panel reinforced at the loaded end perpendicular to the stringer is presented in Appendix C. Although panel C does not have a reinforced end, a comparison is made between the analytical solution and experimental data in Figure 7. Agreement between theory and experiment is not, and was not expected to be, good. The method is presented because it represents another approach to the problem, although for a slightly different configuration.

The stringer-sheet theory is also given in Appendix C. This represents one of the easier theories to apply; however, it can only be applied to the loaded stringer as a quick investigation of the equation will reveal. This analysis was applied to the loaded stringers of panels B and C and the results plotted in Figures 8 and 9 with experimental data. Investigation of the two curves indicates good agreement between theory and experiment, the theoretical solution being slightly non-conservative in one region and slightly conservative in another.

CHAPTER III

CONCLUSIONS

As was stated in Chapter I, the main objective of this study was the comparison of several existing theories of shear lag analysis with experimental data. The conclusions reported in this chapter are based on the comparison of the theoretically predicted normal stresses in the stringers with the experimentally determined normal stresses. The conclusions would probably be different if normal and shearing stresses in the sheet had been included in the analyses and comparisons. The comparisons, reported in Chapter II, led to the conclusion that the best method of analysis consists of a combination of the methods studied rather than any one method by itself. Based on the comparisons reported, the following methods of analysis are suggested:

Based on Accuracy

1. If it is only desired to predict the stresses in the loaded stringer, either the stringer-sheet theory or the substitute-single-stringer theory should be used. The agreement between theory and experiment is about the same for both methods.
2. If it is desired to predict the state of stress in the loaded stringer and approximate the stresses in the adjacent stringers, the substitute-single-stringer method is preferable.
3. If it is desired to predict the stresses in each stringer of the panel, the analysis based on the solution of the differential equations of equilibrium of the normal stresses using minimum potential energy considerations is preferable. The stringer-sheet theory or substitute-single-stringer theory could be used at the same time to predict the stresses in the loaded stringer.

Based on Time Required to Perform Analysis

1. If it is desired to perform a quick analysis, the substitute-single-stringer method is suggested.
2. If it is desired to obtain a more complete picture of the stress distribution in the panel than the substitute-single-stringer method allows, use of the minimum potential energy equations is suggested.
3. The other methods of analysis discussed in the preceeding chapter take much more time to perform than either of the two above and could not be used to perform a quick analysis.

Based on the Type of Structure to Which the Solution is Applicable

1. Since the experimental data used for purposes of comparison was obtained from simple structures, i.e., ones having constant skin thickness and equally spaced stiffeners having the same constant area, a great deal cannot be said about the applicability of the various methods to other structures. It would seem probable, based on the form of equations involved, that the matrix method solution presented in Appendix E would apply to more configurations than would any of the other methods.

Recommendations

Time did not permit a study of all the methods of solution mentioned in Chapter I. Among the methods which have been omitted might be a better method than any reported in this paper. The research reported herein should be continued using the following analytical methods or analogies for comparison:

1. Akao's finite difference equations,

2. Fine's stress function solution,

3. Goland's hydrodynamic analogy,

4. Ross and Newton's electrical analogy,

5. Kuhn's mechanical analog.

The research should be further continued to include the analysis of panels having

1. unequally spaced stiffeners,

2. stiffeners with different areas,

3. variable skin thickness,

4. stiffeners which have areas varying along the length of the panel,

5. skin which varies along the length of the panel,

6. combinations of the above.

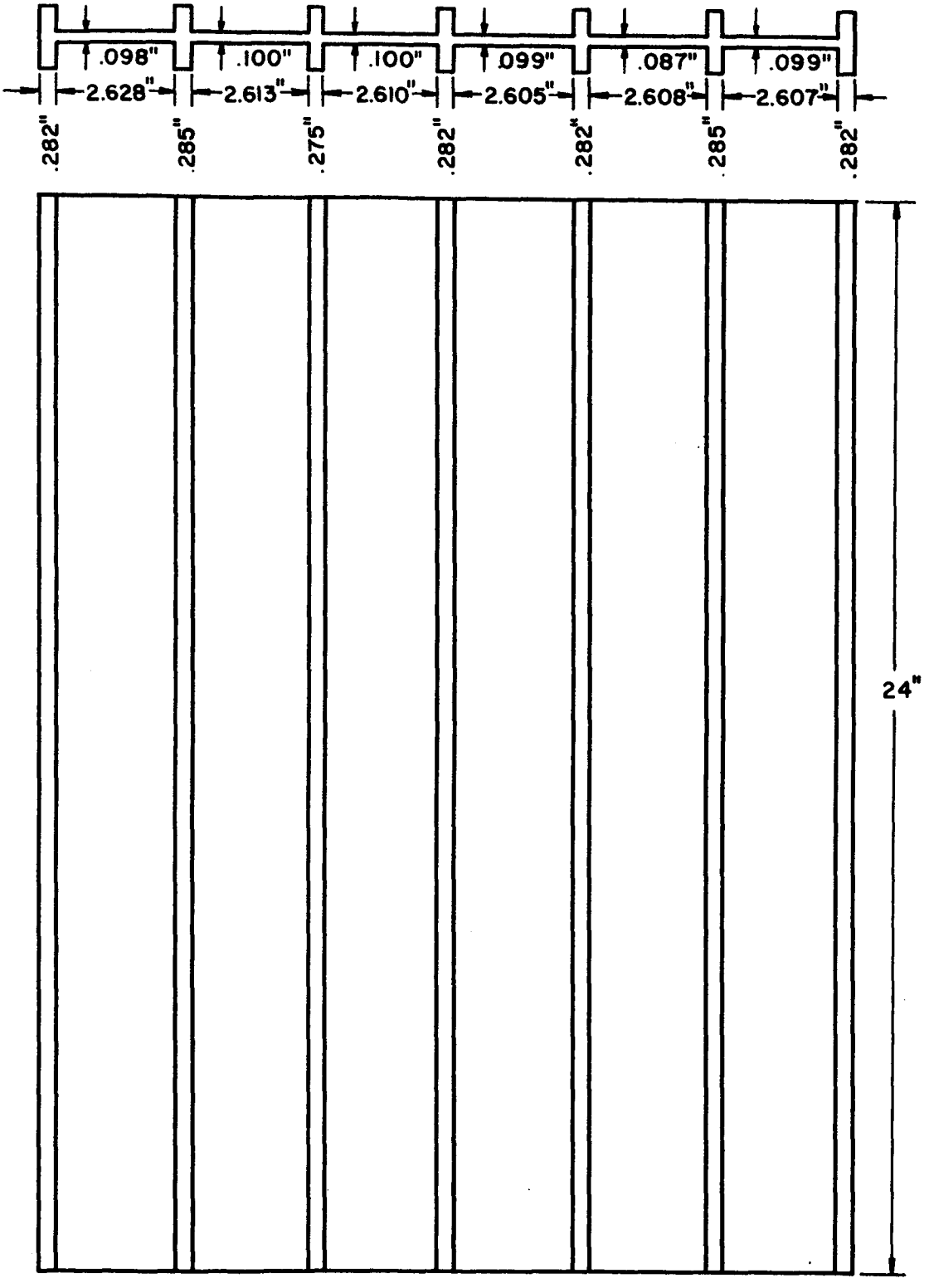

FIGURE 1 PANEL B.

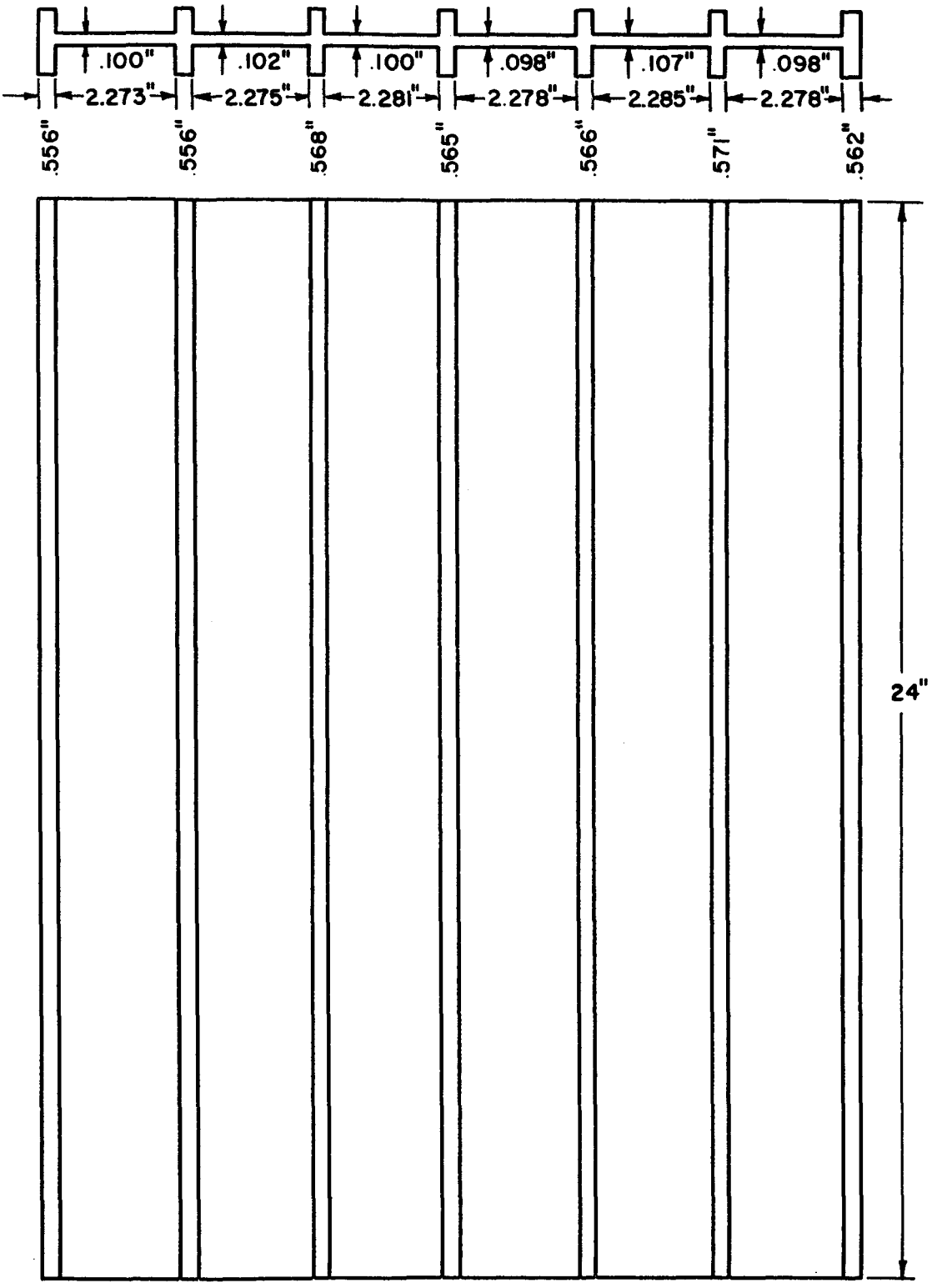

FIGURE 2 PANEL C

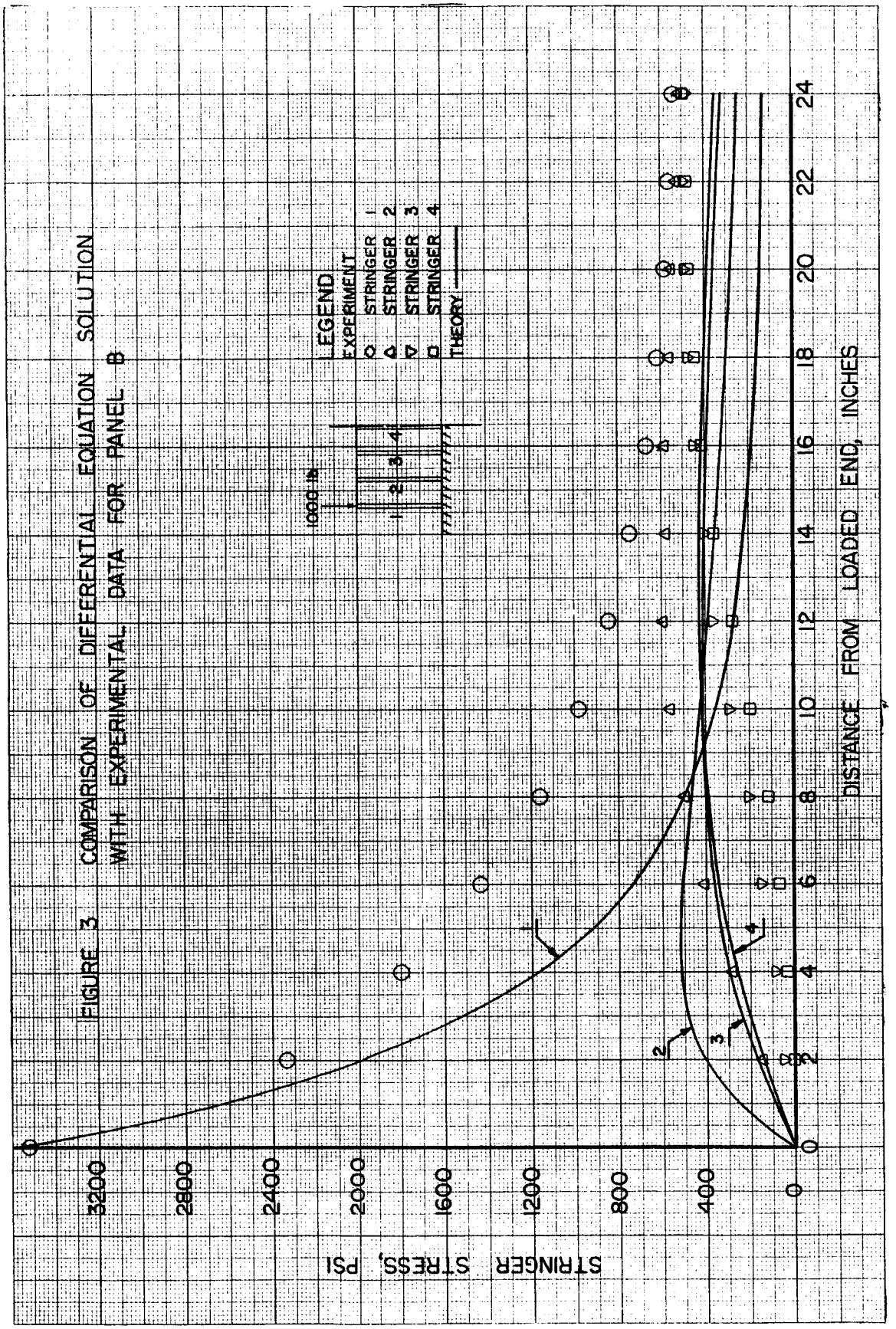
FIGURE 3 COMPARISON OF DIFFERENTIAL EQUATION SOLUTION WITH EXPERIMENTAL DATA FOR PANEL B
LEGEND
EXPERIMENT
STRINGER 1
STRINGER 2
STRINGER 3
STRINGER 4
THEORY
1000 lb
STRINGER STRESS, PSI
DISTANCE FROM LOADED END, INCHES

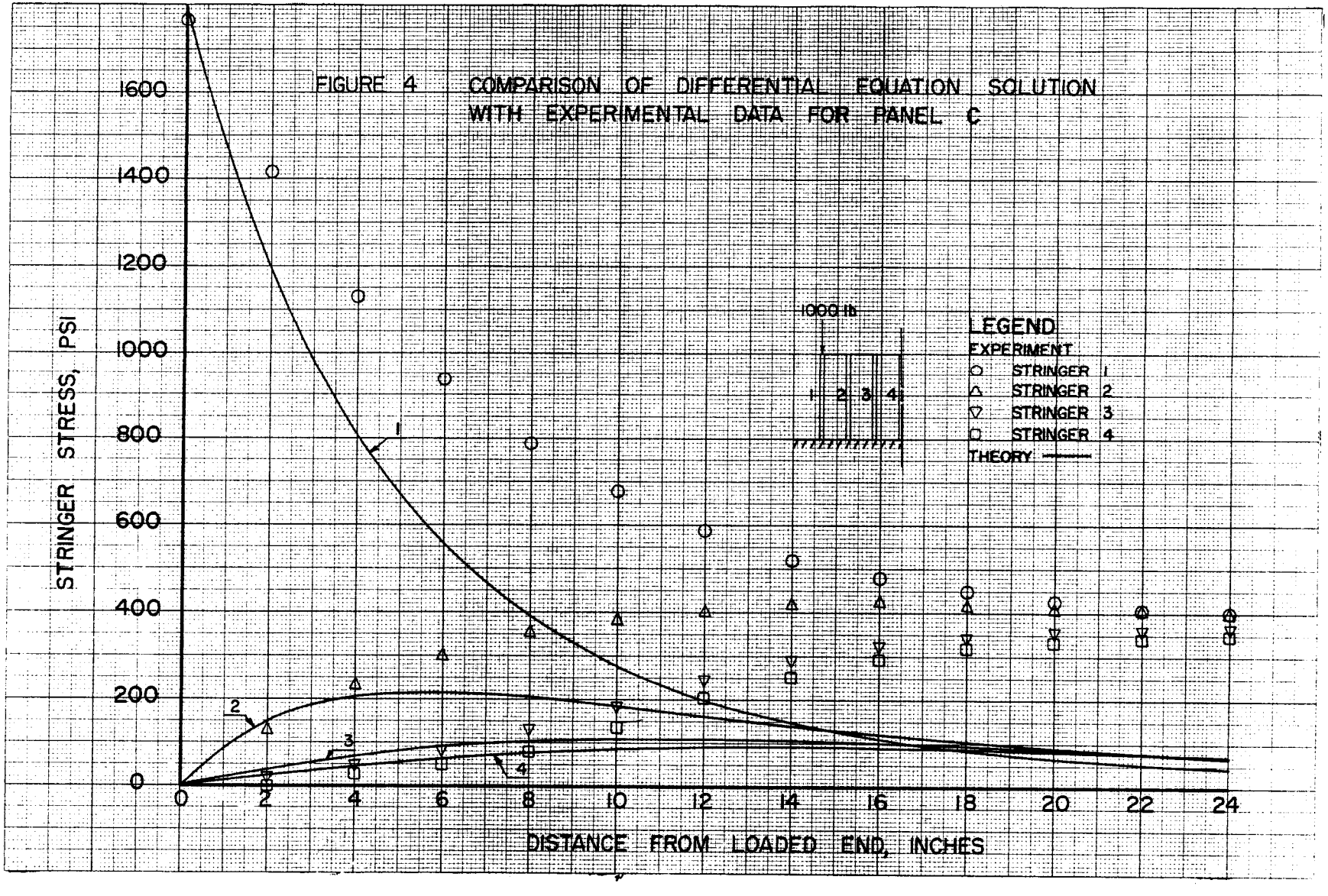
FIGURE 4 COMPARISON OF DIFFERENTIAL EQUATION SOLUTION WITH EXPERIMENTAL DATA FOR PANEL C
STRINGER STRESS, PSI
1600
1400
1200
1000
800
600
400
200
0
0
2
4
6
8
10
12
14
16
18
20
22
24
DISTANCE FROM LOADED END, INCHES
1
2
3
4
1000 lb
1 2 3 4
LEGEND
EXPERIMENT
STRINGER 1
STRINGER 2
STRINGER 3
STRINGER 4
THEORY

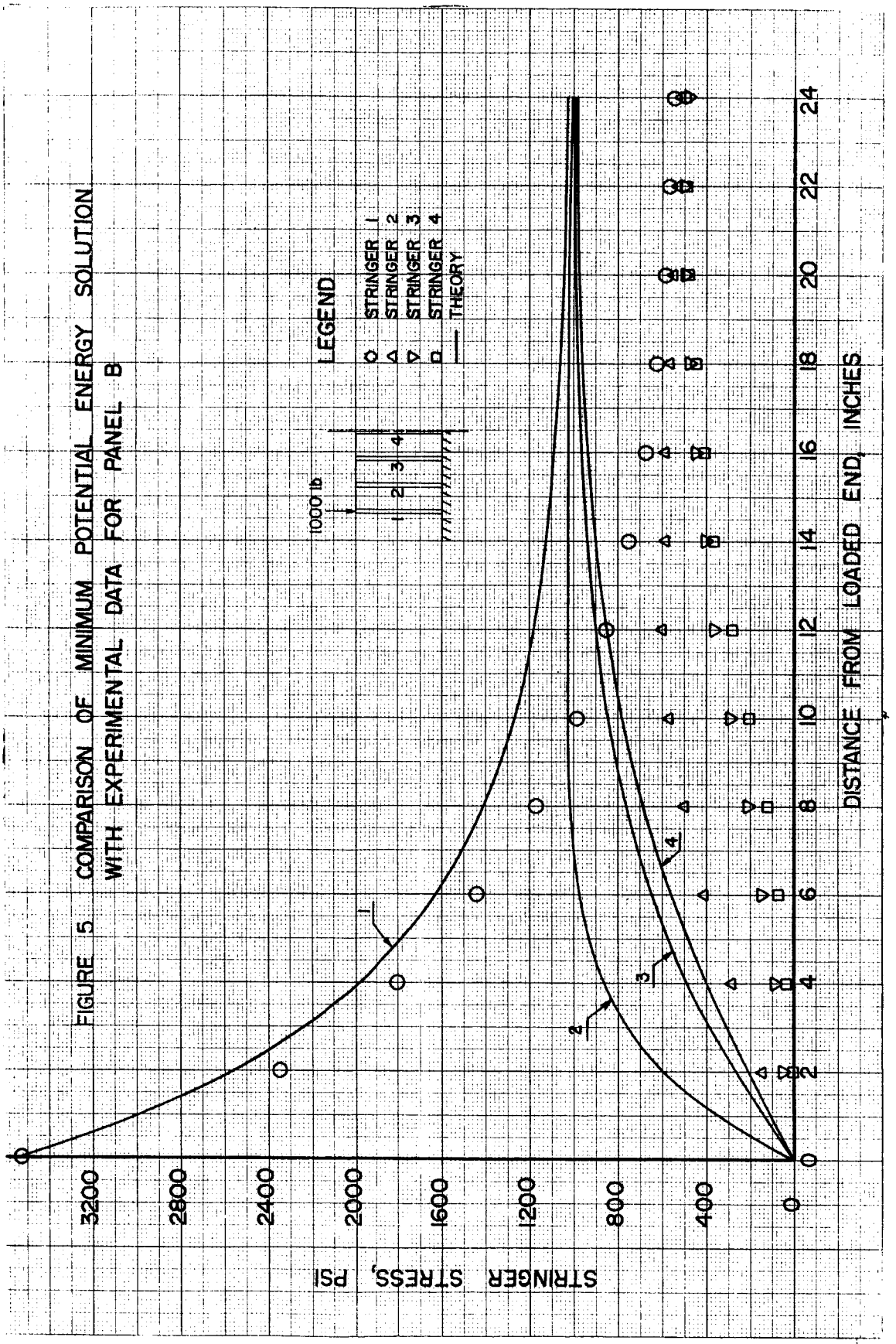

FIGURE 5 COMPARISON OF MINIMUM POTENTIAL ENERGY SOLUTION WITH EXPERIMENTAL DATA FOR PANEL B

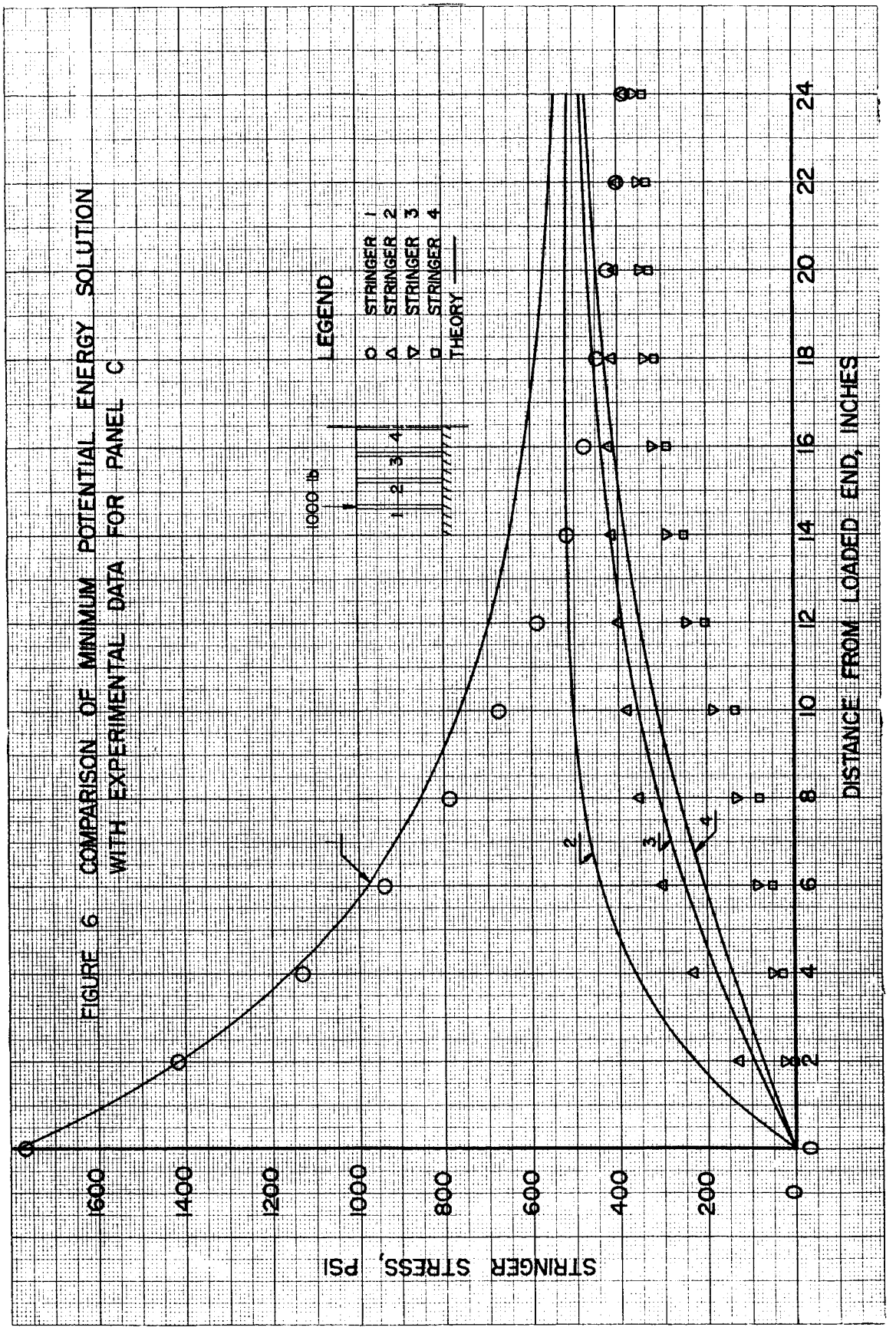

FIGURE 6 COMPARISON OF MINIMUM POTENTIAL ENERGY SOLUTION WITH EXPERIMENTAL DATA FOR PANEL C

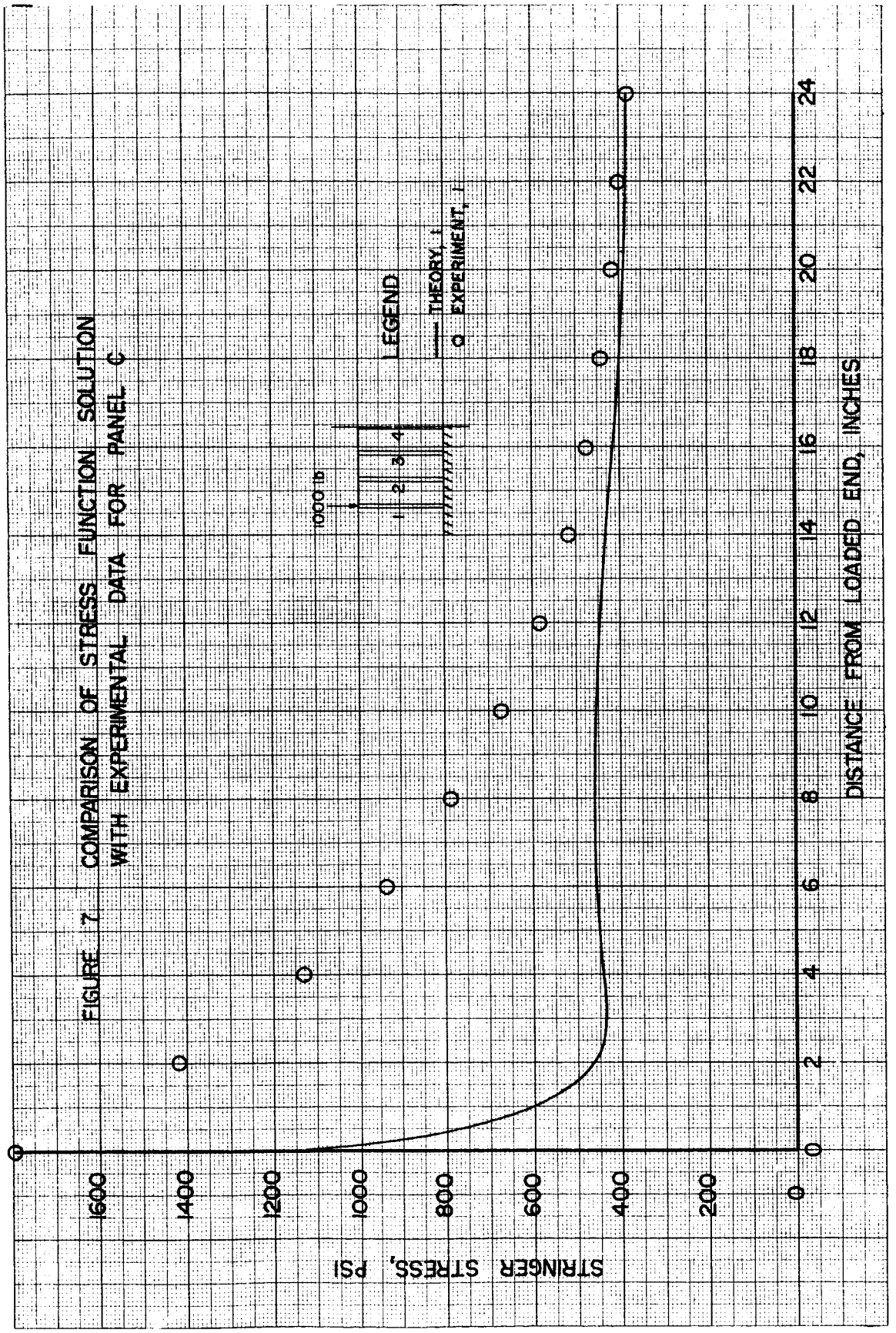

FIGURE 7. COMPARISON OF STRESS FUNCTION SOLUTION WITH EXPERIMENTAL DATA FOR PANEL C

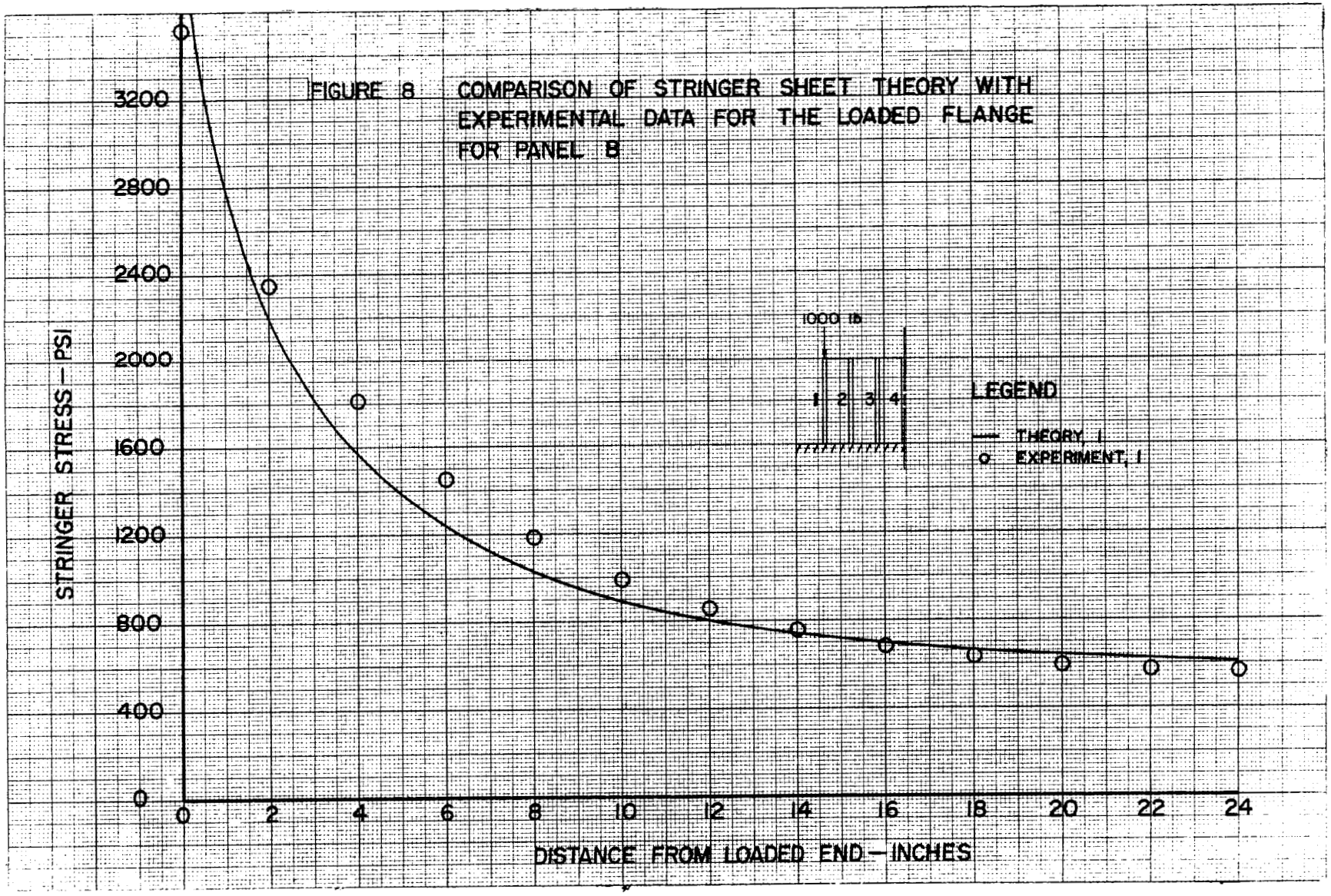

FIGURE 8 COMPARISON OF STRINGER SHEET THEORY WITH EXPERIMENTAL DATA FOR THE LOADED FLANGE FOR PANEL B

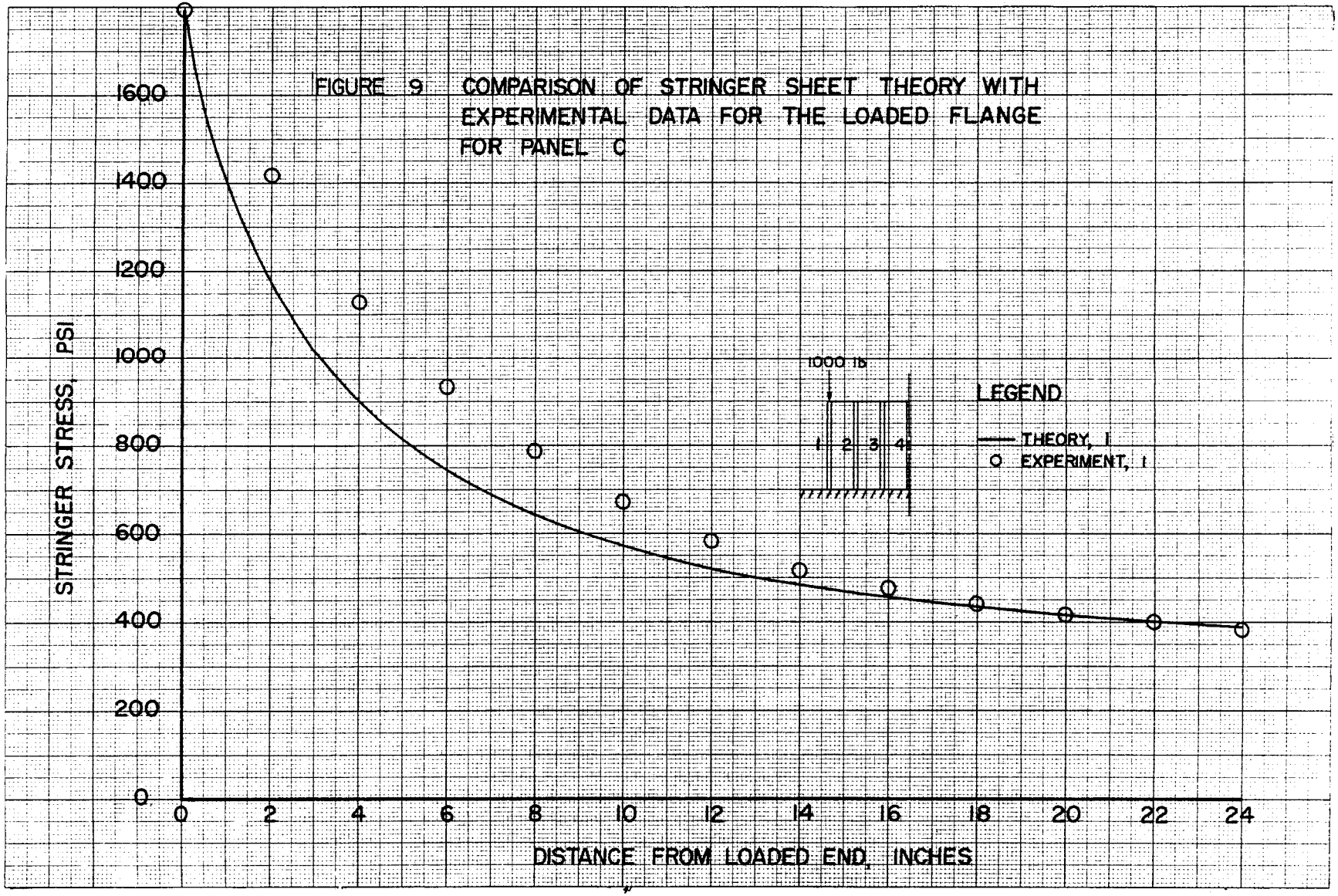
FIGURE 9 COMPARISON OF STRINGER SHEET THEORY WITH EXPERIMENTAL DATA FOR THE LOADED FLANGE FOR PANEL C
STRINGER STRESS, PSI
1600
1400
1200
1000
800
600
400
200
0
0
2
4
6
8
10
12
14
16
18
20
22
24
DISTANCE FROM LOADED END, INCHES
1000 lb
1
2
3
4
LEGEND
THEORY, t
EXPERIMENT, t

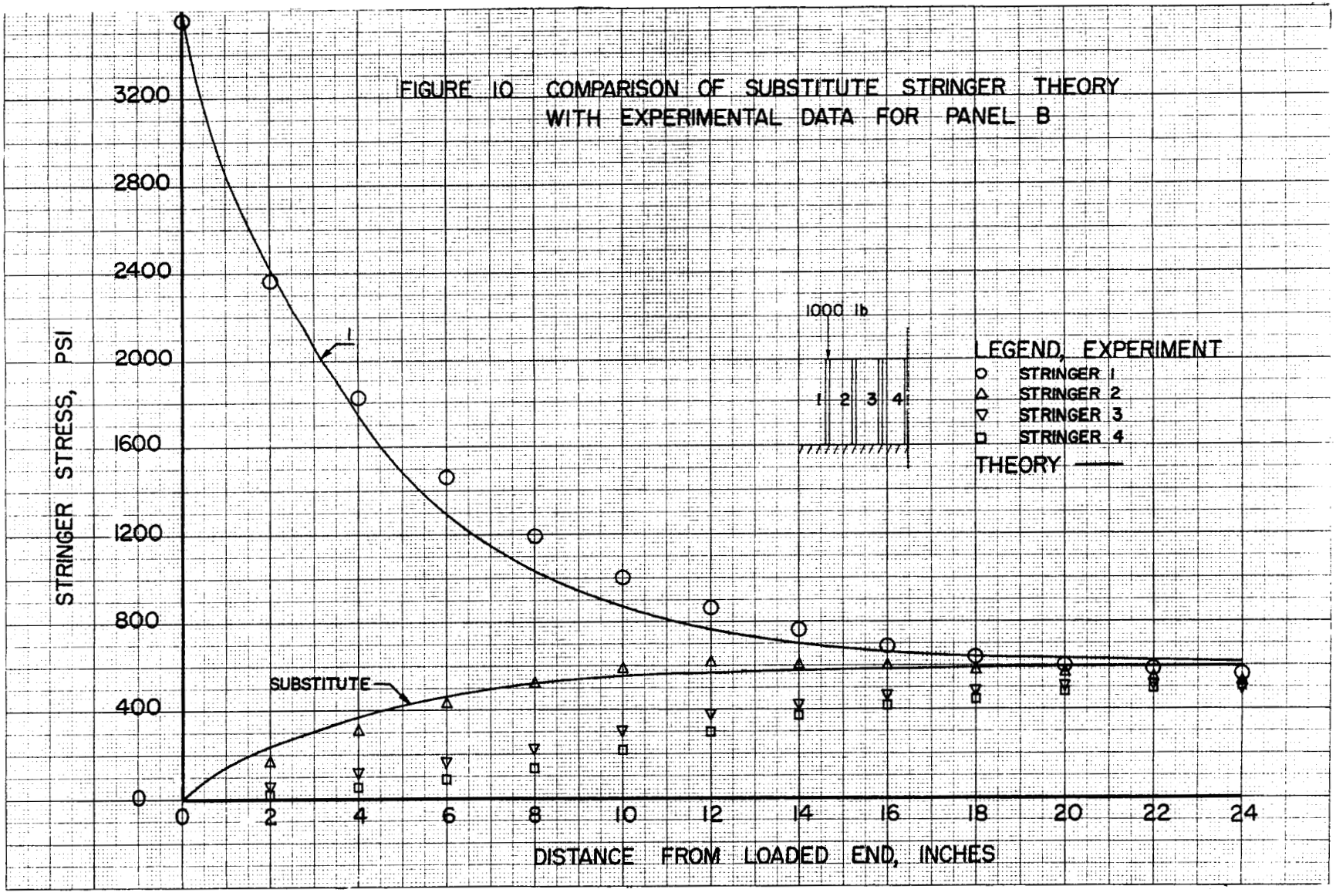
FIGURE 10 COMPARISON OF SUBSTITUTE STRINGER THEORY WITH EXPERIMENTAL DATA FOR PANEL B
STRINGER STRESS, PSI
3200
2800
2400
2000
1600
1200
800
400
0
1
SUBSTITUTE
1000 lb
1 2 3 4
LEGEND, EXPERIMENT
STRINGER 1
STRINGER 2
STRINGER 3
STRINGER 4
THEORY
0 2 4 6 8 10 12 14 16 18 20 22 24
DISTANCE FROM LOADED END, INCHES

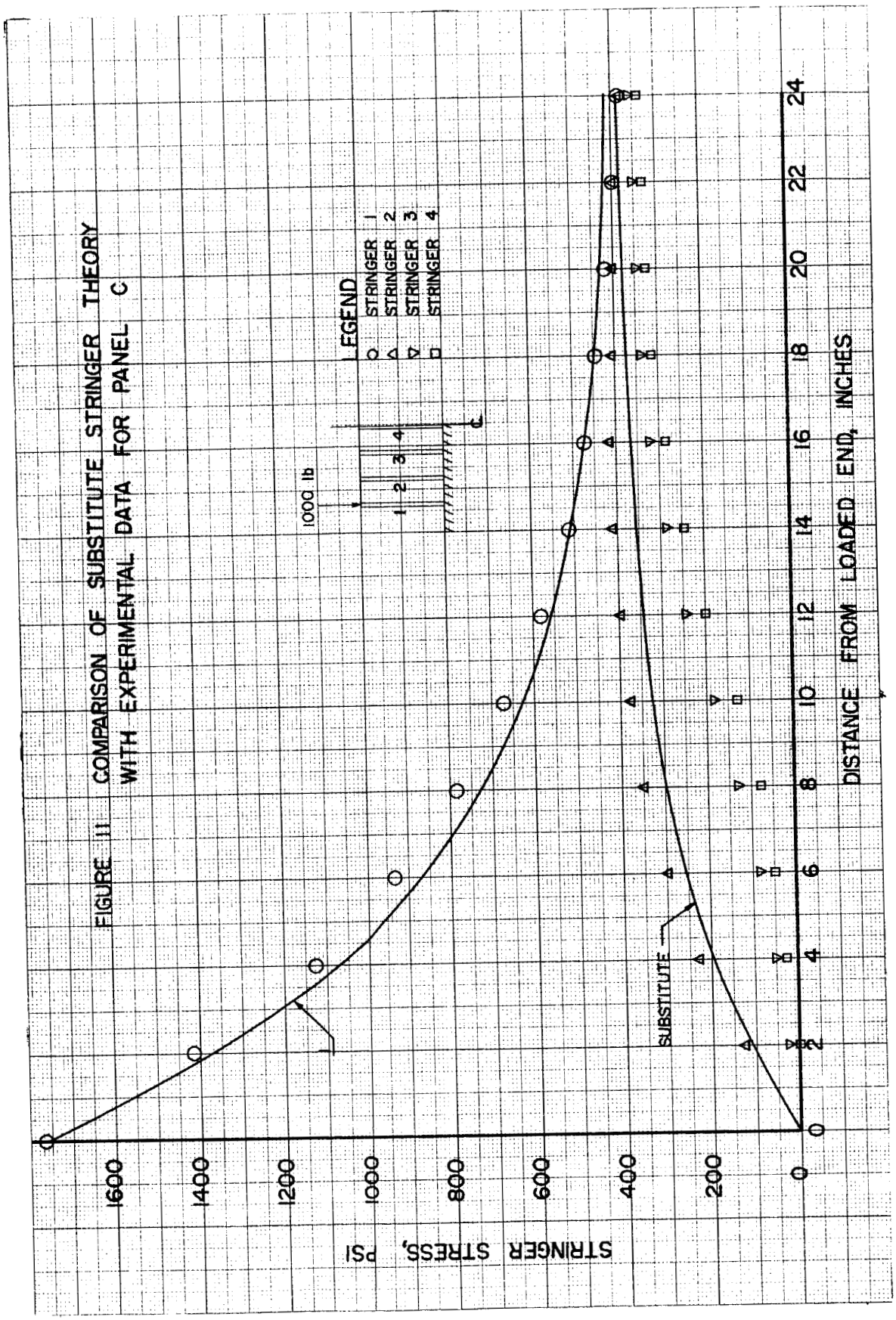
FIGURE 11 COMPARISON OF SUBSTITUTE STRINGER THEORY WITH EXPERIMENTAL DATA FOR PANEL C
LEGEND
STRINGER 1
STRINGER 2
STRINGER 3
STRINGER 4
1000 lb
1 2 3 4
C
STRINGER STRESS, PSI
1600
1400
1200
1000
800
600
400
200
0
SUBSTITUTE
0 2 4 6 8 10 12 14 16 18 20 22 24
DISTANCE FROM LOADED END, INCHES

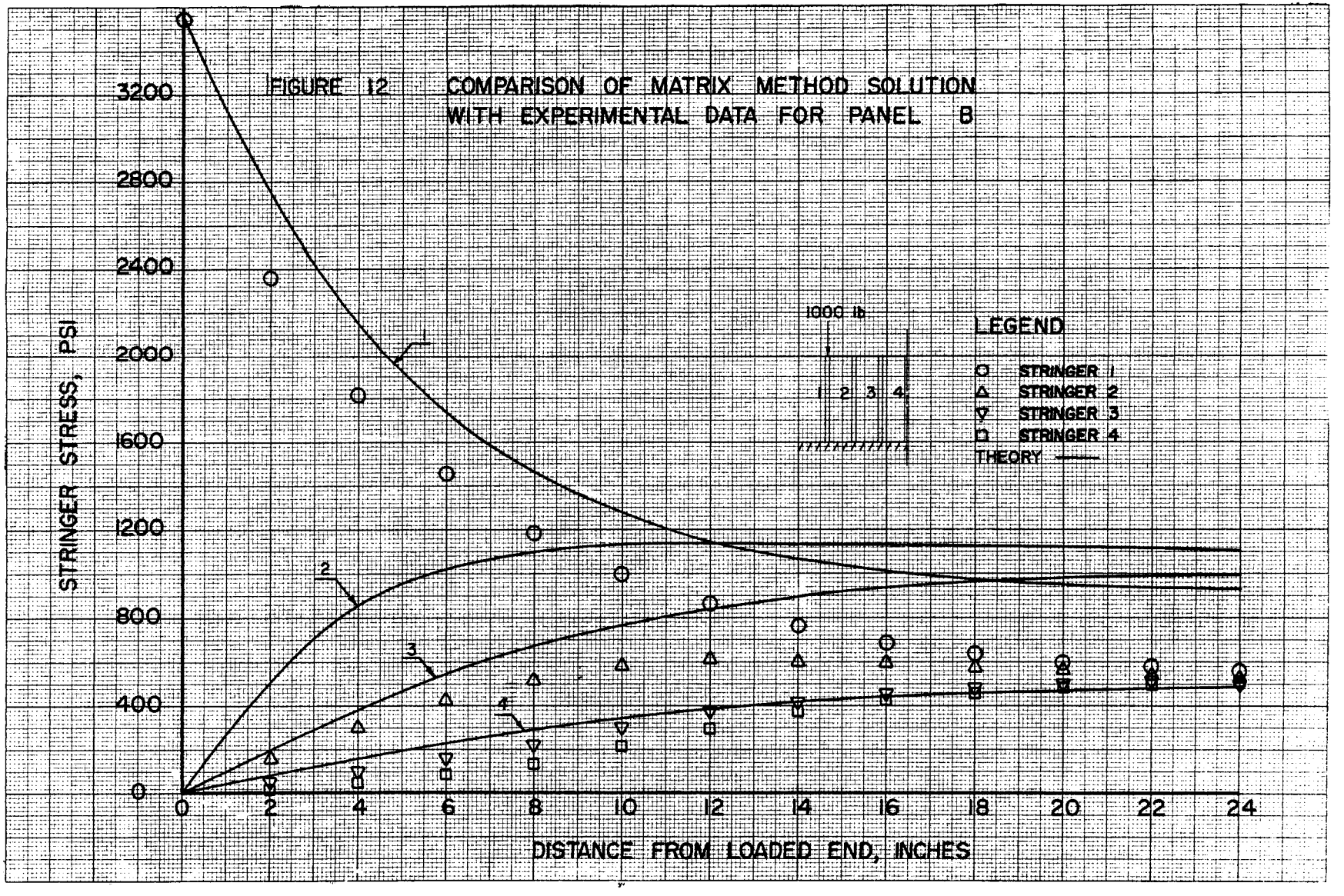
FIGURE 12 COMPARISON OF MATRIX METHOD SOLUTION WITH EXPERIMENTAL DATA FOR PANEL B
STRINGER STRESS, PSI
3200
2800
2400
2000
1600
1200
800
400
0
0
2
4
6
8
10
12
14
16
18
20
22
24
DISTANCE FROM LOADED END, INCHES
1000 lb
1 2 3 4
LEGEND
STRINGER 1
STRINGER 2
STRINGER 3
STRINGER 4
THEORY
1
2
3
4

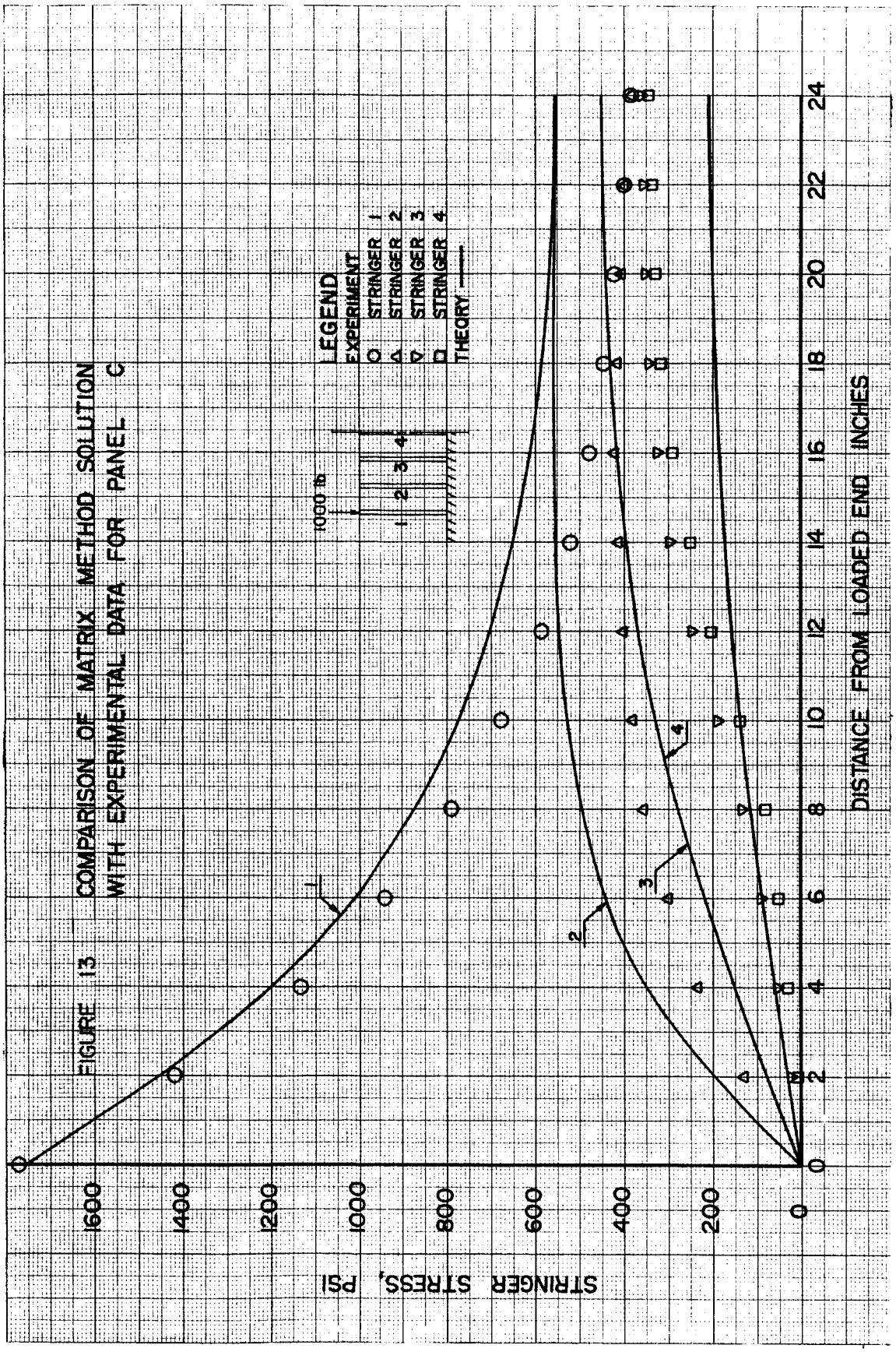

FIGURE 13 COMPARISON OF MATRIX METHOD SOLUTION WITH EXPERIMENTAL DATA FOR PANEL C

APPENDIX A

DIFFERENTIAL EQUATION SOLUTION

Figure A1 represents one-half of a longitudinally stiffened panel, symmetric about the center line, subjected to an axial compressive load on the outer stringer. From Figure A1-b, a free-body diagram of the outer stringer and adjacent sheet, assuming the stringers carry only normal stresses and the sheet carries only shearing stresses, summing forces in the vertical direction,

$$(\sigma_1 + d\sigma_1)A_1 - \tau_1 t dx - \sigma_1 A = 0,$$

or

$$\frac{d\sigma_1}{dx} - \frac{t}{A_1}\tau_1 = 0 . \qquad \text{A1}$$

From A1-c, a free-body diagram of stringer 2,

$$\tau_1 t dx + (\sigma_2 + d\sigma_2)A_2 - \sigma_2 A_2 - \tau_2 t dx = 0 ,$$

or

$$\frac{d\sigma_2}{dx} - \frac{t}{A_2}(\tau_2 - \tau_1) = 0 . \qquad \text{A2}$$

From A1-d, a free-body diagram of stringer 3,

$$\tau_2 t dx + (\sigma_3 + d\sigma_3)A_3 - \sigma_3 A_3 - \tau_3 t dx = 0 ,$$

or

$$\frac{d\sigma_3}{dx} - \frac{t}{A_3}(\tau_3 - \tau_2) = 0 . \qquad \text{A3}$$

In general,

$$\frac{d\sigma_n}{dx} - \frac{t}{A_n}(\tau_n - \tau_{n-1}) = 0 ,$$

or

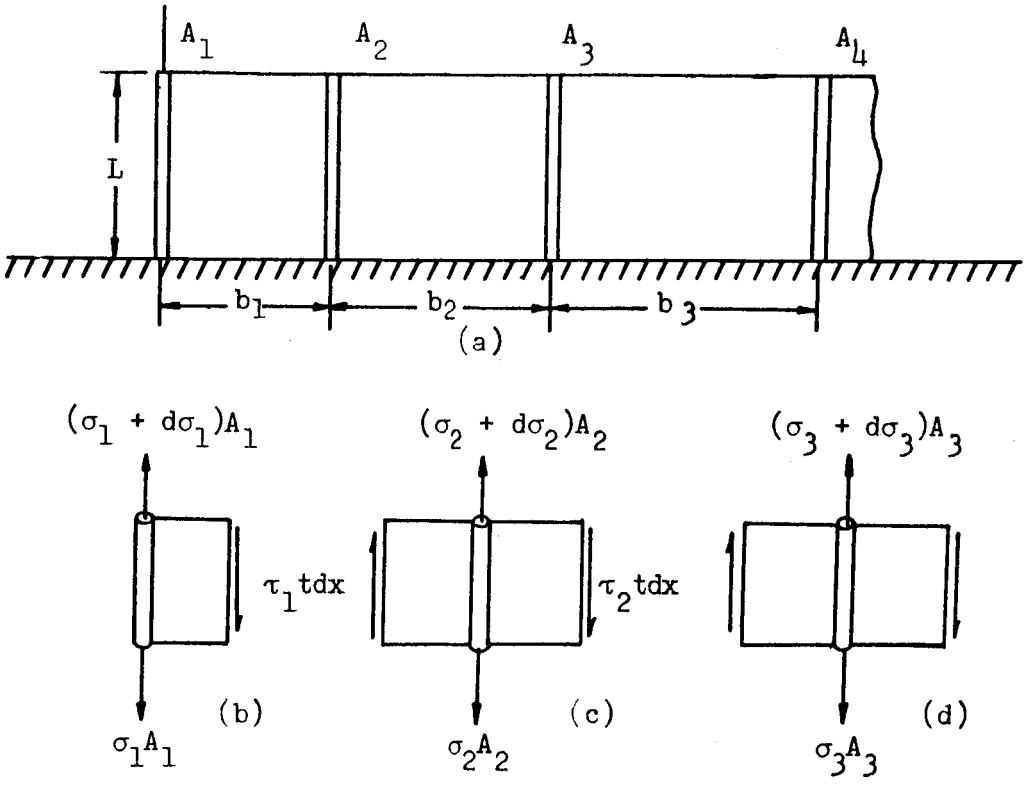

Figure A1--Longitudinally stiffened panel subjected to axial load.

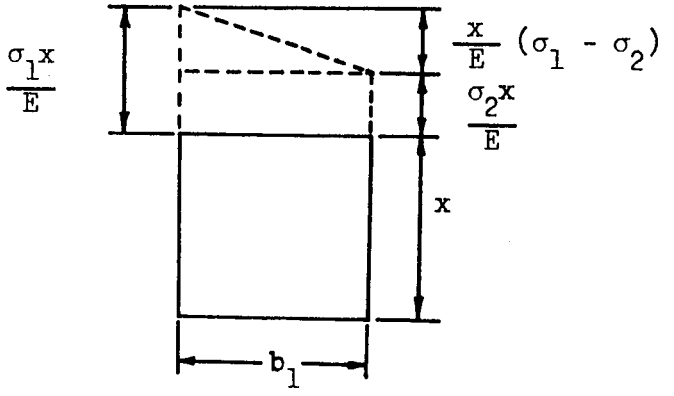

Figure A2--Section of sheet used in determining shear strain.

$$\frac{d\sigma_n}{dx} = \frac{t}{A_n}(\tau_n - \tau_{n-1}) \quad . \qquad \text{A4}$$

Differentiating Equation A4 with respect to x,

$$\frac{d^2\sigma_n}{dx^2} = \frac{t}{A_n}\left[\frac{d\tau_n}{dx} - \frac{d\tau_{n-1}}{dx}\right]. \qquad \text{A5}$$

If we assume $\tan\gamma = \gamma$; then from Figure A2 the shear strain at station x is given by

$$\gamma_1 = \frac{x}{b_1 E}(\sigma_1 - \sigma_2) \quad . \qquad \text{A6}$$

The incrememt of shear strain is

$$d\gamma = \frac{(\sigma_1 - \sigma_2)}{bE}\, dx. \qquad \text{A7}$$

The increment of shear stresses is

$$\frac{d\tau_1}{dx} = \frac{G}{b_1 E}(\sigma_1 - \sigma_2) \quad , \qquad \text{A8}$$

or, in general,

$$\frac{d\tau_n}{dx} = \frac{G}{b_n E}(\sigma_n - \sigma_{n+1}) \quad . \qquad \text{A9}$$

Substituting Equation A9 into Equation A5,

$$\frac{d^2\sigma_n}{dx^2} = \frac{t}{A_n}\left[\frac{G}{b_n E}(\sigma_n - \sigma_{n+1}) - \frac{G}{b_n E}(\sigma_{n-1} - \sigma_n)\right].$$

Assuming b_n = constant = b,

$$\frac{d^2\sigma_n}{dx^2} = \frac{Gt}{bA_n E}\left[2\sigma_n - \sigma_{n+1} - \sigma_{n-1}\right] \quad . \qquad \text{A10}$$

Numerical Example

The value of A_n is determined from the dimensions of the left hand stringer shown in Figure 2. Thus,

$$A_n = (0.556)(1.0) = 0.556.$$

This value is used throughout although the actual areas of the other stringers differ by a small amount. The value of b is given by the distance between the centroid of the left hand stringer and the adjacent stringer. Thus,

$$b = \frac{0.556}{2} + 2.273 + \frac{0.556}{2} = 2.829.$$

The mechanical properties of the material are

$$G = (3.9)(10^6) \text{ psi},$$

$$E = (10.5)(10^6) \text{ psi}.$$

Substituting properties of panel C into Equation A10 for stringer 1, 2, 3, and 4 yields

$$\frac{d^2\sigma_1}{dx^2} = \frac{(3.9)(10^6)(0.1)}{(2.829)(0.556)(10.5)(10^6)}\left[2\sigma_1 - \sigma_2 - \cancel{\sigma_0}^{0}\right]$$

$$\frac{d^2\sigma_1}{dx^2} = 0.04712\sigma_1 - 0.02356\sigma_2 \qquad \text{A11}$$

$$\frac{d^2\sigma_2}{dx^2} = 0.02356[2\sigma_2 - \sigma_3 - \sigma_1]$$

$$= 0.04712\sigma_2 - 0.02356\sigma_3 - 0.02356\sigma_1 \qquad \text{A12}$$

$$\frac{d^2\sigma_3}{dx^2} = 0.02356[2\sigma_3 - \sigma_4 - \sigma_2]$$

$$= 0.04712\sigma_3 - 0.02356\sigma_4 - 0.02356\sigma_2 \qquad \text{A13}$$

$$\frac{d^2\sigma_4}{dx^2} = 0.02356[2\sigma_4 - \sigma_5 - \sigma_3] .$$

Since the panel has 7 stringers and is symmetric about the center line,

$\sigma_5 = \sigma_3$ by symmetry.

$$\frac{d^2\sigma_4}{dx^2} = 0.04712\sigma_4 - 0.04712\sigma_3 \ . \qquad \text{A14}$$

Writing Equations A11, A12, A13 and A14 in matrix notation

$$D^2 \begin{bmatrix} \sigma_1 \\ \sigma_2 \\ \sigma_3 \\ \sigma_4 \end{bmatrix} = \begin{bmatrix} .04712 & -.02356 & 0 & 0 \\ -.02356 & .04712 & -.02356 & 0 \\ 0 & -.02356 & .04712 & -.02356 \\ 0 & 0 & -.04712 & .04712 \end{bmatrix} \begin{bmatrix} \sigma_1 \\ \sigma_2 \\ \sigma_3 \\ \sigma_4 \end{bmatrix} \qquad \text{A15}$$

where D^2 denotes $\frac{d^2}{dx^2}$:

The characteristic equation is obtained from the matrix

$$\begin{bmatrix} 0.04712 - \lambda & -0.02356 & 0 & 0 \\ -0.02356 & 0.04712 - \lambda & -0.02356 & 0 \\ 0 & -0.02356 & 0.04712 - \lambda & -0.02356 \\ 0 & 0 & -0.04712 & 0.04712 - \lambda \end{bmatrix}$$

setting its determinant equal to zero

$$\begin{vmatrix} 1 - \zeta & -1/2 & 0 & 0 \\ -1/2 & 1 - \zeta & -1/2 & 0 \\ 0 & -1/2 & 1 - \zeta & -1/2 \\ 0 & 0 & -1 & 1 - \zeta \end{vmatrix} = 0$$

where $\zeta = \frac{\lambda}{0.04712}$.

Expanding the determinant

$$\zeta^4 - 4\zeta^3 + 5\zeta^2 - 2\zeta + 0.125 = 0. \qquad \text{A16}$$

The roots to Equation A16 are

$$\zeta_1 = 0.6103445$$

$\zeta_2 = 0.0761025$

$\zeta_3 = 1.9135555$

$\zeta_4 = 1.3999975$

so that

$\lambda_1 = 0.02875943$

$\lambda_2 = 0.00358594$

$\lambda_3 = 0.09016673$

$\lambda_4 = 0.06596788$

The solution to Equation A15 is

$$\begin{bmatrix} \sigma_1 \\ \sigma_2 \\ \sigma_3 \\ \sigma_4 \end{bmatrix} = \left[e^{-\sqrt{M}\,x} \right] \begin{bmatrix} k_1 \\ k_2 \\ k_3 \\ k_4 \end{bmatrix} \qquad \text{A17}$$

where M is the coefficient matrix of Equation A15. The term $e^{-\sqrt{M}\,x}$ is most easily determined from the relation

$$e^{-\sqrt{M}\,x} = e^{-\sqrt{\lambda_1}\,x} z_1 + e^{-\sqrt{\lambda_2}\,x} z_2 + e^{-\sqrt{\lambda_3}\,x} z_3 + e^{-\sqrt{\lambda_4}\,x} z_4 \qquad \text{A18}$$

where the z's are given by

$$(\lambda_1 - \lambda_2)(\lambda_1 - \lambda_3)(\lambda_1 - \lambda_4) z_1 = (M - \lambda_2 I)(M - \lambda_3 I)(M - \lambda_4 I) \qquad \text{A19}$$

$$(\lambda_2 - \lambda_1)(\lambda_2 - \lambda_3)(\lambda_2 - \lambda_4) z_2 = (M - \lambda_1 I)(M - \lambda_3 I)(M - \lambda_4 I) \qquad \text{A20}$$

$$(\lambda_3 - \lambda_1)(\lambda_3 - \lambda_2)(\lambda_3 - \lambda_4) z_3 = (M - \lambda_1 I)(M - \lambda_2 I)(M - \lambda_4 I) \qquad \text{A21}$$

$$(\lambda_4 - \lambda_1)(\lambda_4 - \lambda_2)(\lambda_4 - \lambda_3) z_4 = (M - \lambda_1 I)(M - \lambda_2 I)(M - \lambda_3 I) \qquad \text{A22}$$

where I is the unit matrix.

Performing the calculations indicated in Equations A19-A22,

$$z_1 = \begin{bmatrix} 0.43689435 & 0.31665946 & -0.17716203 & -0.22736339 \\ 0.31665946 & 0.25973232 & -0.13806731 & -0.17716203 \\ -0.17716203 & -0.13806731 & 0.08257029 & 0.08929606 \\ -0.45472678 & -0.35432402 & 0.17859217 & 0.25973235 \end{bmatrix} \quad \text{A23}$$

$$z_2 = \begin{bmatrix} 0.06816075 & 0.13602883 & 0.17771962 & 0.09618382 \\ 0.13602883 & 0.24588038 & 0.32839648 & 0.17771962 \\ 0.17771962 & 0.32839648 & 0.42360001 & 0.23221266 \\ 0.19236764 & 0.35543923 & 0.46442530 & 0.24588037 \end{bmatrix} \quad \text{A24}$$

$$z_3 = \begin{bmatrix} 0.06863274 & -0.13604887 & 0.18572910 & -0.10164644 \\ -0.13604887 & 0.25436184 & -0.33934175 & 0.18572910 \\ 0.18572910 & -0.33934175 & 0.44009096 & -0.23769531 \\ -0.20329288 & 0.37145820 & -0.47539065 & 0.25436184 \end{bmatrix} \quad \text{A25}$$

$$z_4 = \begin{bmatrix} 0.42631324 & -0.31663507 & -0.18628016 & 0.23282548 \\ -0.31663507 & 0.24003309 & 0.14901589 & -0.18628016 \\ -0.18628016 & 0.14901589 & 0.05375296 & -0.08380958 \\ 0.46565096 & -0.37256030 & -0.16761910 & 0.24003311 \end{bmatrix} \quad \text{A26}$$

At $x = 0$,

$$e^{-\sqrt{M}x} = I.$$

So that equation A17 becomes

$$\begin{bmatrix} \sigma_1 \\ \sigma_2 \\ \sigma_3 \\ \sigma_4 \end{bmatrix} = \begin{bmatrix} 1 & 0 & 0 & 0 \\ 0 & 1 & 0 & 0 \\ 0 & 0 & 1 & 0 \\ 0 & 0 & 0 & 1 \end{bmatrix} \begin{bmatrix} k_1 \\ k_2 \\ k_3 \\ k_4 \end{bmatrix} \quad \text{A27}$$

Also at $x = 0$,

$$\sigma_1 = \frac{P}{A} \approx 1800$$

$$\sigma_2 = \sigma_3 = \sigma_4 = 0.$$

Therefore, from Equation A27

$$k_1 = 1800$$

$$k_2 = 0$$

$$k_3 = 0$$

$$k_4 = 0.$$

The solution of Equation A15 is thus

$$\begin{bmatrix}\sigma_1\\ \sigma_2\\ \sigma_3\\ \sigma_4\end{bmatrix} = \Bigg(e^{-0.16958605x}\begin{bmatrix} 0.43689435 & 0.31665946 & -0.17716203 & -0.22736339\\ 0.31665946 & 0.25973232 & -0.13806731 & -0.17716203\\ -0.17716203 & -0.13806731 & 0.08257029 & 0.08929606\\ -0.45472678 & -0.35432402 & 0.17859217 & 0.25973235\end{bmatrix}$$

$$+ e^{-0.059882718x}\begin{bmatrix} 0.06816075 & 0.13602883 & 0.17771962 & 0.09618382\\ 0.13602883 & 0.24588038 & 0.32839648 & 0.17771962\\ 0.17771962 & 0.32839648 & 0.42360001 & 0.23221266\\ 0.19236764 & 0.35543923 & 0.46442530 & 0.24588037\end{bmatrix}$$

$$+ e^{-0.30027775x}\begin{bmatrix} 0.06863274 & -0.13604887 & 0.18572910 & -0.10164644\\ -0.13604887 & 0.25436184 & -0.33934175 & 0.18572910\\ 0.18572910 & -0.33934175 & 0.44009096 & -0.23769531\\ -0.20329288 & 0.37145820 & -0.47539065 & 0.25436184\end{bmatrix}$$

$$+ e^{-0.25684213x}\begin{bmatrix} 0.42631324 & -0.31663507 & -0.18628016 & 0.23282548\\ -0.31663507 & 0.24003309 & 0.14901589 & -0.18628016\\ -0.18628016 & 0.14901589 & 0.05375296 & -0.08380958\\ 0.46565096 & -0.37256030 & -0.16761910 & 0.24003311\end{bmatrix}\Bigg)\begin{bmatrix}1800\\ 0\\ 0\\ 0\end{bmatrix}$$

or

$$\sigma_1 = [0.43689435e^{-0.16958605x} + 0.06816075e^{-0.059882718x} + 0.06863274e^{-0.30027775x} + 0.42631324e^{-0.25684213x}] 1800$$

$$\sigma_2 = [0.31665946e^{-0.16958605x} + 0.13602883e^{-0.059882718x} + 0.13604887e^{-0.30027775x} + 0.31663507e^{-0.25684213x}] 1800$$

$$\sigma_3 = [-0.17716203e^{-0.16958605x} + 0.17771962e^{-0.059882718x} + 0.18572910e^{-0.30027775x} - 0.18628016e^{-0.25684213x}] 1800$$

$$\sigma_4 = [-0.45472678e^{-0.16958605x} + 0.19236764e^{-0.059882718x} - 0.20329288e^{-0.30027775x} + 0.46565096e^{-0.25684213x}] 1800$$

The stresses obtained from the above solution is plotted in Figure 4 with experimental data.

APPENDIX B

MINIMUM POTENTIAL ENERGY EQUATIONS

Goodey [13] presented an analysis of the diffusion of an end load into a panel with (2N-1) stringers. In this solution, the stringers are treated as discrete members separated by panels of skin which transmit only shear stresses.

The panel considered is shown in Figure B1 where the notation used is also given.

Following is an outline of the analysis:

1. Considering elements of the stringers and longerons, differential equations of equilibrium of the forces were obtained.
2. Equations from step 1 were integrated from x to ∞.
3. The differential equation for the total strain energy, U, for half the complete panel was derived.
4. Conditions of minimum strain energy were then obtained by applying the method of the calculus of variations to the integral for U, resulting in N independent equations. These equations were then substituted into the results of step 2 yielding a set of second order differential equations.
5. A solution was assumed for the equations in step 4.
6. Through the use of boundary conditions, various trigonometric identities, and algebraic manipulations, the constants of integration were evaluated.
7. The final solutions were presented as follows:

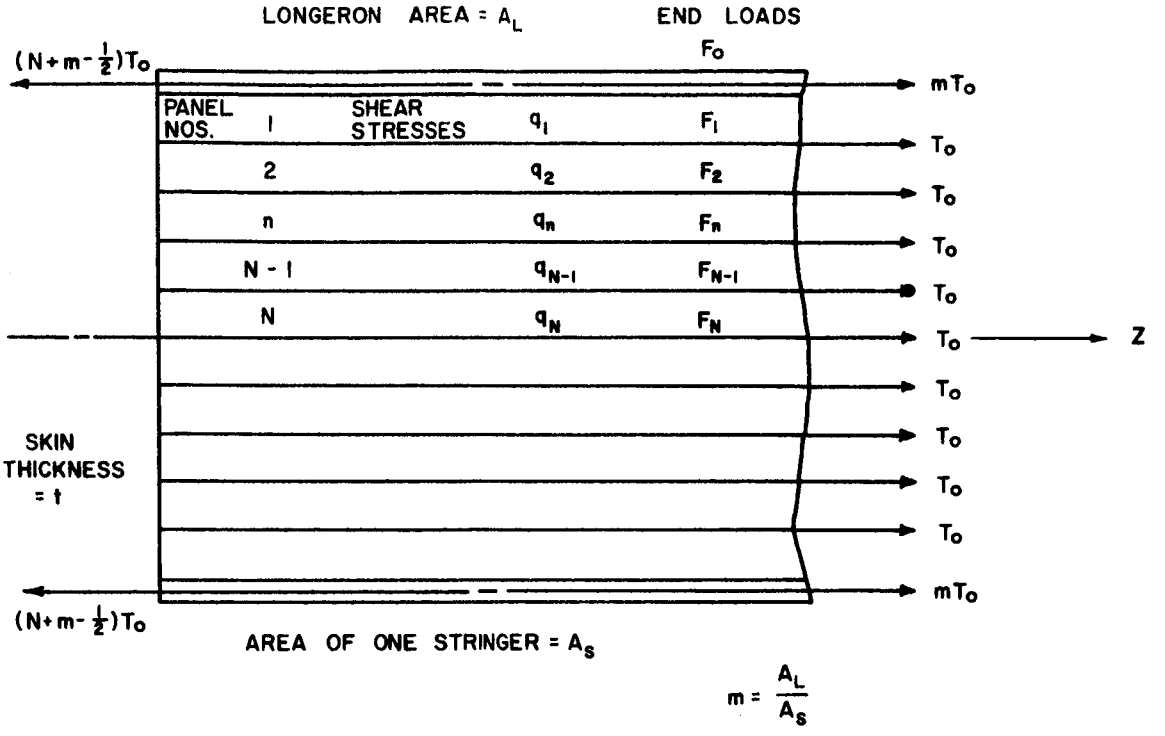

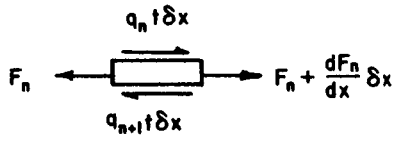

ELEMENT OF n^{th} STRINGER

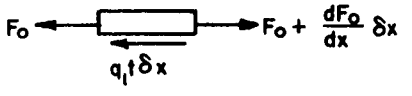

ELEMENT OF LONGERON OR EDGE MEMBER

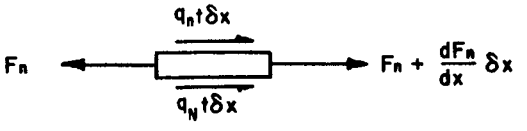

ELEMENT OF N^{th} STRINGER

FIGURE B1 NOTATION USED IN MINIMUM POTENTIAL ENERGY SOLUTION.

$$\frac{F_o}{T_\infty} = m - \left(N + m - \frac{1}{2}\right) \cdot$$

$$\sum_{r=1}^{r=N} \frac{[\cos(2N\varphi_r)\sin(2N-1)\varphi_r]\, e^{-2kx(\sin\varphi_r)}}{\sin\varphi_r \left[N + \dfrac{m - \frac{1}{2}}{1+4m(m-1)\sin^2\varphi_r}\right]} \qquad \text{B2}$$

$$\frac{F_n}{T_\infty} = 1 + (2N + 2M - 1) \cdot$$

$$\sum_{r=1}^{r=N} \frac{[\cos(2N\varphi_r)\cos2(N-n)\varphi_r]\, e^{-2kx(\sin\varphi_r)}}{N + \dfrac{m - \frac{1}{2}}{1+4m(m-1)\sin^2\varphi_r}} \qquad \text{B3}$$

$n = 1, 2, 3, \ldots, N$

where $m = \dfrac{A_L}{A_S}$, $k = \left[\dfrac{Gt}{bEA_S}\right]^{1/2}$, $\varphi_r = \dfrac{r}{2N+1}$, r = 1 to N.

For the special case when m = 1 the above equations reduced to

$$\frac{F_o}{T_\infty} = 1 + 2\sum_{r=1}^{r=N} \cos^2\varphi_r\, e^{-2kx\sin\varphi_r} \qquad \text{B4}$$

$$\frac{F_n}{T_\infty} = 1 + 2\sum_{r=1}^{r=N} \cos\varphi_r \cos(2N+1)\varphi_r\, e^{-2kx\sin\varphi_r} \qquad \text{B5}$$

Numerical Example

Consider panel C as shown in Figure 2. It is assumed that the stiffener areas are the same and that b = 2.84 = constant, t = 0.1 = constant. This panel is, according to Goodey's nomenclature, a 5 stringer, 2 longeron panel. Thus

$$2N-1 = 5 ,$$

$$N = 3 .$$

Since the areas of the stiffeners are assumed to be equal, the ratio of longeron area to stringer area is

$$m = \frac{A_L}{A_S} = 1$$

so equations B4 and B5 can be used. Remembering

$$\varphi_r = \frac{r\pi}{2N+1} = \frac{r\pi}{7} \text{ radians.}$$

so that

$$\frac{F_o}{T_\infty} = 1 + 2\sum_{r=1}^{3} \cos^2\varphi_r e^{-2kx\sin\varphi_r}$$

$$= 1 + 2\left(\cos^2\varphi_1 e^{-2kx\sin\varphi_1} + \cos^2\varphi_2 e^{-kx\sin\varphi_2} + \cos^2\varphi_3 e^{-2kx\sin\varphi_3}\right). \qquad B6$$

Substituting the value of φ_r into Equation B6,

$$\frac{F_o}{T_\infty} = 1 + 2\left(0.811945e^{-0.86836kx} + 0.388939e^{-1.5634kx} + 0.049461e^{-1.97489kx}\right). \qquad B7$$

Using Eq. B5 for stringer 1,

$$\frac{F_1}{T_\infty} = 1 + 2\sum_{r=1}^{3} \cos\varphi_r \cos 3\varphi_r e^{-2kx\sin\varphi_r} .$$

Substituting the value of φ_r,

$$\frac{F_1}{T_\infty} = 1 + 2\left(0.199576e^{-0.86836kx} - 0.561796e^{-1.5634kx} - 0.138925e^{-1.94978kx}\right). \qquad B8$$

Using Eq. B5 for stringer 2

$$\frac{F_2}{T_\infty} = 1 + 2\sum_{r=1}^{r=3} \cos\varphi_r \cos 5\varphi_r e^{-2kx\sin\varphi_r} .$$

Substituting the value of φ_r,

$$\frac{F_2}{T_\infty} = 1 + 2\left(-0.561589e^{-0.86836kx} - 0.138874e^{-1.5634kx} + 0.200652e^{-1.94478kx}\right). \qquad B9$$

Likewise for stringer 3

$$\frac{F_3}{T_\infty} = 1 + 2\left(-0.90082e^{-0.86836kx} + 0.62365e^{-1.5634kx} - 0.22268e^{-1.94978kx}\right). \qquad B10$$

Equations B7, B8, B9, and B10 apply to any 7 stringer panel with m = 1 and b and t constant. Thus they can be used for the analysis of panel B as well as C, the only difference being in the value of k.

Numerical evaluation of the above equations was performed at increments of x = 1 inch from x = 0 to x = 24. To expedite these calculations, a digital computer program was written for the Univac Solid State 80 which is on the University of Alabama's main campus. The machine language used was Bama-Bell II which is a floating point mathematical interpretative system for the USS 80.[2]

The program used follows:

```
200     I556901000
201     I506901000
202     0600000000
203     0800000005
204     I201100109
205     6400400000
206     3400109300
```

[2]Gray, William J.: Bama-Bell II, Floating Point Mathematical Interpretative System for USS 80 System. University of Alabama Computer Center.

207	3103300301	
208	R601301301	
209	3106301301	
210	3104300302	
211	R601302302	
212	3107302302	
213	3105300303	
214	R601303303	
215	3108303303	
216	1301302302	
217	1302303303	
218	3102303401	
219	1101401401	
220	3401100401	
221	I241400401	
222	1101400400	
223	7000023206	
224	7000003202	
225	I260000000	
226	R403000000	
zzz	200	Note: the z's must be a double punch nine over eight.

Writing the equations to be evaluated in the general form

$$\frac{F_n}{T_\infty} = 1 + 2\left(C_1 e^{-0.86836kx} + C_2 e^{-1.5634kx} + C_3 e^{-1.97489kx}\right),$$

the following shows the necessary data locations for use of the above given program:

100	T_∞	(in floating point)

101	5010000000	
102	5020000000	
103	4986836000	(negative)
104	5015634000	(negative)
105	5019497800	(negative)
106	C_1	(in floating point)
107	C_2	(in floating point)
108	C_3	(in floating point)
109	k	(in floating point)

The print out, in floating point, is of the form:

x	f(x)
x_1	$f(x_1)$
x_2	$f(x_2)$
.	.
.	.
.	.
5124000000	f(24)

For panel C having a 1000 load on each longeron,

$$T_\infty = \frac{2000}{2(0.5557)+2(0.5632)+2(0.5618)+0.5612} = 509.86$$

$$k = \left[\frac{(3.9)(10^6)(0.1)}{(10.5)(10^6)(2.84)(0.555)}\right]^{1/2} = 0.15355.$$

Equations B7, B8, B9 and B10 are shown plotted in Figure 6 along with experimental data for comparison.

APPENDIX C

STRESS FUNCTION SOLUTION

Goodey [13] presented a stress function type solution for the analysis of a plane sheet reinforced in two directions at right angles. This analysis was as follows:

Referring to Figure C1, the following equations were obtained for the stiffeners.

$$\varepsilon_x = \frac{1}{E}(\sigma_x - \mu\sigma_y) \qquad C1$$

$$\varepsilon_y = \frac{1}{E}(\sigma_y - \mu\sigma_x) \qquad C2$$

$$G = \frac{E}{2(1+\mu)} = \frac{\tau_{xy}}{\varepsilon_{xy}} \; . \qquad C3$$

Defining the average normal stress as

$$\frac{P_{sheet} + P_{stiffener}}{A_{sheet} + A_{stiffener}} \; ,$$

the average stress in direction O_x is

$$\frac{t\sigma_x + t_x(\sigma_x - \mu\sigma_y)}{t + tx} = P_x \qquad C4$$

and the average stress in direction O_y is

$$\frac{t\sigma_y + ty(\sigma_y - \mu\sigma_x)}{t + ty} = P_y \; . \qquad C5$$

Defining

$$k_x = 1 + \frac{tx}{t}, \quad tk_x = t + tx \qquad C6$$

and

$$k_y = 1 + \frac{t_y}{t} \; , \quad tk_y = t + ty. \qquad C7$$

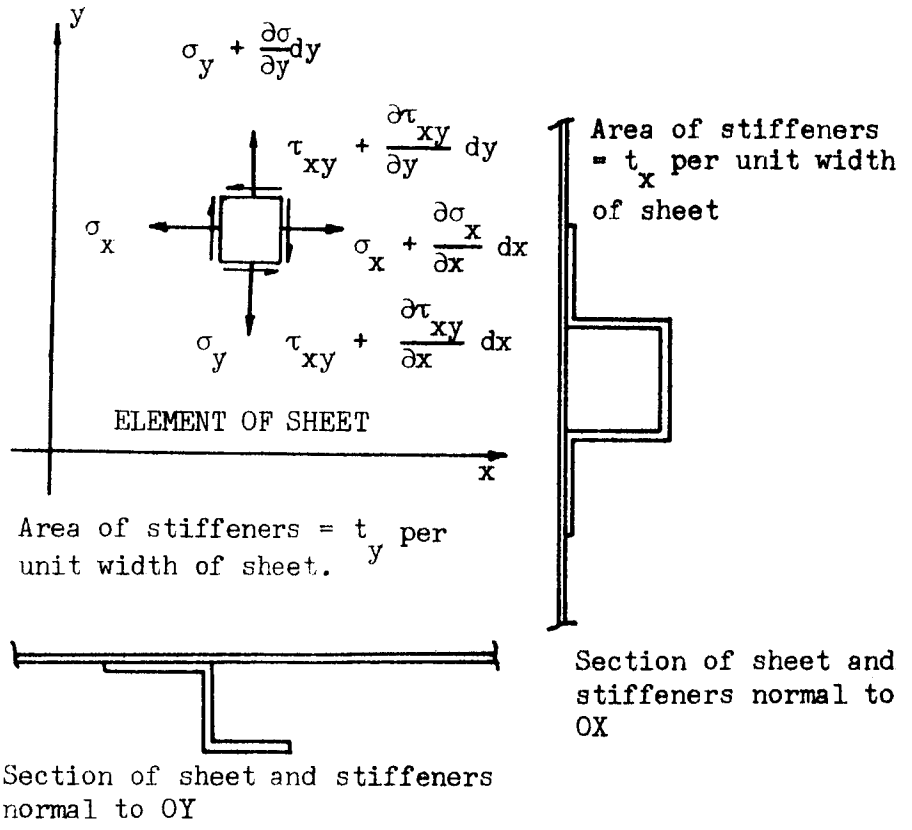

Figure C1-- Diagram of plain sheet reinforced in two directions at right angles.

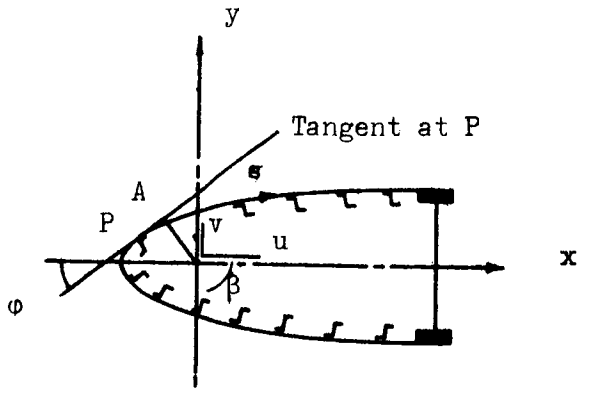

Figure C2--View of cross-section looking along OZ in positive direction of Z.

Substituting Equations C6 and C7 into Equations C4 and C5, yields, after some manipulation,

$$P_x = \sigma_x - \mu\sigma_y\left(1 - \frac{1}{k_x}\right) \qquad C8$$

$$P_y = \sigma_y - \mu\sigma_x\left(1 - \frac{1}{k_y}\right).$$

Distributing the area of the stiffeners in the x direction uniformly over the sheet results in the free-body diagrams of Figure C2

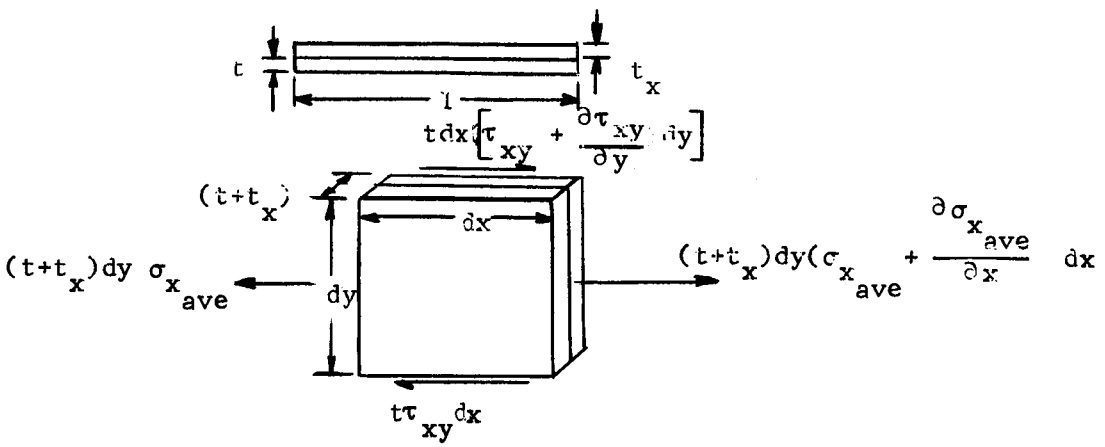

Figure C2 - Free-body showing forces in x direction acting on element of sheet and stringer

Summation of forces in the x direction yields

$$(t + t_x)\frac{\partial \sigma_{x_{ave}}}{\partial x} + t\frac{\partial \tau_{xy}}{\partial y} = 0. \qquad C10$$

Substituting Equation C4 into Equation C10 for $\sigma_{x_{ave}}$ results in

$$\frac{\partial}{\partial x}\ \sigma_x t + (\sigma_x - \mu\sigma_y)t_x\ + t\frac{\partial \tau_{xy}}{\partial y} = 0. \qquad C11$$

From Equation C4,

$$\frac{\partial}{\partial x}\ \partial_x t + (\partial_x - \mu\partial_y)t_x\ + t\frac{\partial \tau_{xy}}{\partial y} = \frac{\partial}{\partial x}\ P_x(t+t_x)\ + t\frac{\partial \tau_{xy}}{\partial y}$$

$$= t\frac{\partial \tau_{xy}}{\partial y} + \frac{\partial}{\partial x}(P_x k_x t) \qquad C12$$

so that

$$t\frac{\partial \tau_{xy}}{\partial y} + \frac{\partial}{\partial x}\left(tP_x k_x\right) = 0$$

or

$$\frac{\partial \tau_{xy}}{\partial y} + k_x \frac{\partial P_x}{\partial x} = 0. \qquad C13$$

Similarly, the area of the stiffeners in the y direction may be distributed and forces summed in the y direction. The following equation results

$$\frac{\partial \tau_{xy}}{\partial x} + k_y \frac{\partial P_y}{\partial y} = 0. \qquad C14$$

Equations C13 and C14 are satisfied if we express the stresses in terms of a stress function Φ, where

$$\tau_{xy} = -\frac{\partial^2 \Phi}{\partial x \partial y} \qquad C15$$

$$P_x = \frac{1}{k_x}\frac{\partial^2 \Phi}{\partial y^2} \qquad C16$$

$$P_y = \frac{1}{k_y}\frac{\partial^2 \Phi}{\partial x^2}\,. \qquad C17$$

Substituting Equation C8 into Equation C1, Equation C9 into Equation C2, and rewriting Equation C3 yields

$$E\varepsilon_x = P_x - P_y\frac{\mu}{k_x} \qquad C18$$

$$E\varepsilon_y = P_y - P_x\frac{\mu}{k_y}$$

$$E\varepsilon_{xy} = 2(1 + \mu)\tau_{xy}\,. \qquad C20$$

Now, using the relations,

$$\varepsilon_x = \frac{\partial u}{\partial x}$$

$$\varepsilon_y = \frac{\partial v}{\partial y}$$

$$\varepsilon_{xy} = \frac{\partial v}{\partial x} + \frac{\partial u}{\partial y}$$

$$P_x = \frac{1}{k_x}\frac{\partial^2 \Phi}{\partial y^2}$$

$$P_y = \frac{1}{k_y}\frac{\partial^2 \Phi}{\partial x^2}$$

$$\tau_{xy} = -\frac{\partial^2 \Phi}{\partial x \partial y}$$

and substituting into Equations C18, C19, and C20,

$$E\frac{\partial u}{\partial x} = \frac{1}{k_x}\frac{\partial^2 \Phi}{\partial y^2} - \frac{\mu}{k_x}\frac{1}{k_y}\frac{\partial^2 \Phi}{\partial x^2}\ , \qquad \text{C21}$$

$$E\frac{\partial v}{\partial y} = \frac{1}{k_y}\frac{\partial^2 \Phi}{\partial x^2} - \frac{\mu}{k_y}\frac{1}{k_x}\frac{\partial^2 \Phi}{\partial y^2}\ , \qquad \text{C22}$$

$$E\left(\frac{\partial v}{\partial x} + \frac{\partial u}{\partial y}\right) = 2(1 + \mu)\left(-\frac{\partial^2 \Phi}{\partial x \partial y}\right)\ . \qquad \text{C23}$$

Differentiating Equation C21 twice with respect to y,

$$E\frac{\partial^3 u}{\partial x \partial y^2} = \frac{1}{k_x}\frac{\partial^4 \Phi}{\partial y^4} - \frac{\mu}{k_x k_y}\frac{\partial^4 \Phi}{\partial x^2 \partial y^2}\ . \qquad \text{C24}$$

Differentiating Equation C22 twice with respect to x,

$$E\frac{\partial^3 v}{\partial y \partial x^2} = \frac{1}{k_y}\frac{\partial^4 \Phi}{\partial x^4} - \frac{\mu}{k_x k_y}\frac{\partial^4 \Phi}{\partial y^2 \partial x^2}\ . \qquad \text{C25}$$

Adding Equations C24 and C25 then substituting Equation C23 yields

$$\frac{1}{k_y}\frac{\partial^4 \Phi}{\partial x^4} + 2\left[1 + \mu\left(1 - \frac{1}{k_x k_y}\right)\right]\frac{\partial^4 \Phi}{\partial x^2 \partial y^2} + \frac{1}{k_x}\frac{\partial^4 \Phi}{\partial y^4} = 0\ . \qquad \text{C26}$$

If $k_x = k_y = 1$, this equation reduces to the familiar equation $\nabla^4 \Phi = 0$ for a plane un-reinforced sheet.

Assume a solution of Equation C26 of the form

$$\Phi = (A\cosh\alpha_1\lambda y + B\cosh\alpha_2\lambda y)\sin\lambda x \qquad C27$$

where α_1 and α_2 satisfy the equation

$$\frac{\alpha^4}{k_x} - 2\left[1 + \mu(1 - \frac{1}{k_x k_y})\right]\alpha^2 + \frac{1}{k_y} = 0 , \qquad C28$$

or

$$\frac{\alpha_1^2}{k_x}, \frac{\alpha_2^2}{k_x} = 1 + \mu(1 - \frac{1}{k_x k_y}) \pm \sqrt{\left[1 + \mu(1 - \frac{1}{k_x k_y})\right]^2 - \frac{1}{k_x k_y}} ; \qquad C29$$

and A and B are constants.

The stresses are now given by the equations

$$-\tau_{xy} = \frac{\partial^2\Phi}{\partial x\partial y} = \lambda^2\cos\lambda x\left(A\alpha_1\sinh\alpha_1\lambda y + B\alpha_2\sinh\alpha_2\lambda y\right) , \qquad C30$$

$$k_x P_x = \frac{\partial^2\Phi}{\partial y^2} = \lambda^2\sin\lambda x\left(A\alpha_1^2\cosh\alpha_1\lambda y + B\alpha_2^2\cosh\alpha_2\lambda y\right) , \qquad C31$$

$$k_y P_y = \frac{\partial^2\Phi}{\partial x^2} = -\lambda^2\sin\lambda x\left(A\cosh\alpha_1\lambda y + B\cosh\alpha_2\lambda y\right) . \qquad C32$$

In order to satisfy the condition $P_y = 0$ when $y = \pm a$, it is necessary that

$$A\cosh\alpha_1\lambda a + B\cosh\alpha_2\lambda a = 0$$

or

$$\frac{A}{\cosh\alpha_2\lambda a} = -\frac{B}{\cosh\alpha_1\lambda a} = k(\lambda) . \qquad C33$$

Substitution into Equations C27, C30, C31, and C32 yields

$$\Phi = k(\lambda)\left[(\cosh\alpha_2\lambda a)(\cosh\alpha_1\lambda y) - (\cosh\alpha_1\lambda a)(\cosh\alpha_2\lambda y)\right]\sin\lambda x, \qquad C34$$

$$-\tau_{xy} = \lambda^2 k(\lambda)\left[(\alpha_1\cosh\alpha_2\lambda a)(\sinh\alpha_1\lambda y) - (\alpha_2\cosh\alpha_1\lambda a)(\sinh\alpha_2\lambda y)\right]\cosh\lambda x, \qquad C35$$

$$k_x P_x = \lambda^2 k(\lambda)\left[(\alpha_1{}^2\cosh\alpha_2\lambda a)(\cosh\alpha_1\lambda y) - (\alpha_2{}^2\cosh\alpha_1\lambda a)(\cosh\alpha_2\lambda y)\right]\sin\lambda x, \quad \text{C36}$$

$$k_y P_y = -\,{}^2k(\lambda)\left[(\cosh\alpha_2\lambda a)(\cosh\alpha_1\lambda y) - (\cosh\alpha_1\lambda a)(\cosh\alpha_2\lambda y)\right]\sin\lambda x\ . \quad \text{C37}$$

The end load in the skin from y = 0 to y = a is given by

$$\int_o^a P_x k_x t\,dy = \lambda t k(\lambda)\left[(\alpha_1\cosh\alpha_2\lambda a)(\sinh\alpha_1\lambda a) - (\alpha_2\cosh\alpha_1\lambda a)(\sinh\alpha_2\lambda a)\right]\sin\lambda x, \quad \text{C38}$$

and the end load in one flange is given by

$$(A_F P_x)_{y=a} = \frac{A_F{}^2 k(\lambda)}{k_x}\left[(\alpha_1{}^2 - \alpha_2{}^2)(\cosh\alpha_1\lambda a)(\cosh\alpha_2\lambda a)\right]\sin\lambda x. \quad \text{C39}$$

If $2T_o$ is the total end load, integration with respect to λ from 0 to ∞ yields

$$\frac{2T_o}{\pi} = \int_0^\infty \lambda t k(\lambda)\left[(\alpha_1\cosh\alpha_2\lambda a)(\sinh\alpha_1\lambda a) - (\alpha_2\cosh\alpha_1\lambda a)(\sinh\alpha_2\lambda a) + \frac{A_F}{k_x t}(\alpha_1{}^2 - \alpha_2{}^2)(\cosh\alpha_1\lambda a)(\cosh\alpha_2\lambda a)\right]\sin\lambda x\,d\lambda\ . \quad \text{C40}$$

If T_o is constant, it may be represented by the integral

$$\frac{2T_o}{\pi}\int_o^\infty \frac{\sin\lambda x}{\lambda}\,d\lambda\ . \quad \text{C41}$$

Since the two integrals must be the same,

$$k(\lambda) = \frac{2T_o a}{\pi t x}\left[\frac{1}{\alpha_1\lambda a(\cosh\alpha_2\lambda a)(\sinh\alpha_1\lambda a) - \alpha_2\lambda a(\cosh\alpha_1\lambda a)(\sinh\alpha_2\lambda a) + m\lambda^2 a^2(\alpha_1{}^2 - \alpha_2{}^2)(\cosh\alpha_1\lambda a)(\cosh\alpha_2\lambda a)}\right] \quad \text{C42}$$

where $m = \frac{A_F}{a k_x t}$. Therefore

$$\Phi = \frac{2T_o a}{t} \int_o^\infty \frac{(\cosh\alpha_2\lambda a)(\cosh\alpha_1\lambda y) - (\cosh\alpha_1\lambda a)(\cosh\alpha_2\lambda y)\ \sin\lambda x d\lambda}{\left[\begin{array}{l}\alpha_1\lambda a(\cosh\alpha_2\lambda a)(\sinh\alpha_1\lambda a) - \alpha_2\lambda a(\cosh\alpha_1\lambda a)(\sinh\alpha_2\lambda a) \\ + m\lambda^2 a^2(\alpha_1^2 - \alpha_2^2)(\cosh\alpha_1\lambda a)(\cosh\alpha_2\lambda a)\end{array}\right]\lambda} \quad \text{C43}$$

Letting $\theta = \lambda a$, Equation C43 may be simplified in appearance becoming

$$\Phi = \frac{2T_o a}{\pi t} \int_o^\infty \left[\frac{\cosh\frac{\alpha_1\theta y}{a}}{\cosh\alpha_1\theta} - \frac{\cosh\frac{\alpha_2\theta y}{a}}{\cosh\alpha_2\theta y}\right] \cdot \left[\frac{\frac{1}{\theta^2}\sin\frac{\theta x}{a}\, d\theta}{\alpha_1\tanh\alpha_1\theta - \alpha_2\tanh\alpha_2\theta + m(\alpha_1^2 - \alpha_2^2)\theta}\right] . \quad \text{C44}$$

Evaluation of this integral was accomplished using the theory of residues. The result obtained was

$$\Phi = \frac{T_o a}{t}\left[\frac{(y^2-a^2)}{2a^2(1+m)} - 2\sum \frac{\frac{\cos\frac{\alpha_1\theta_n y}{a}}{\cos\alpha_1\theta_n} - \frac{\cos\frac{\alpha_2\theta_n y}{a}}{\cos\alpha_2\theta_n}\ e^{-\frac{\theta_n x}{a}}}{\theta_n^2\ \alpha_1^2\sec^2\alpha_1\theta_n - \alpha_2^2\sec^2\alpha_2\theta_n - m(\alpha_1^2-\alpha_2^2)}\right] \quad \text{C45}$$

where the coefficients θ_n are roots of the equation

$$\alpha_1\tan\alpha_1\theta - \alpha_2\tan\alpha_2\theta + m(\alpha_1^2 - \alpha_2^2)\theta = 0 . \quad \text{C46}$$

The stresses are now obtained from Equation C45 by differentiation. Letting $T_o = p_o a k_x t(1+m)$ where p_o is the uniform stress at $x = \infty$, the stresses are

$$\tau_{xy} = -\frac{\partial^2\Phi}{\partial x \partial y} = 2P_o k_x(1+m)\sum \frac{\left[\frac{\alpha_1\sin\frac{\alpha_1\theta_n y}{a}}{\cos\alpha_1\theta_n} - \frac{\alpha_2\sin\frac{\alpha_2\theta_n y}{a}}{\cos\alpha_2\theta_n}\right] e^{-\frac{\theta_n x}{a}}}{\alpha_1^2\sec^2\alpha_1\theta_n - \alpha_2^2\sec_2\alpha_2\theta_n + m(\alpha_1^2-\alpha_2^2)} , \quad \text{C47}$$

$$P_x = \frac{1}{k_x}\frac{\partial^2\Phi}{\partial y^2} = P_o + 2P_o(1+m)\sum \frac{\left[\frac{\alpha_1^2\cos\frac{\alpha_1\theta_n y}{a}}{\cos\alpha_1\theta_n} - \frac{\alpha_2^2\cos\frac{\alpha_2\theta_n y}{a}}{\cos\alpha_2\theta_n}\right] e^{-\frac{\theta_n x}{a}}}{\alpha_1^2\sec^2\alpha_1\theta_n - \alpha_2^2\sec^2\alpha_2\theta_n + m(\alpha_1^2-\alpha_2^2)}, \qquad C48$$

$$P_y = \frac{1}{k_y}\frac{\partial^2\Phi}{\partial x^2} = -\frac{2P_o k_x(1+m)}{k_y}\sum \frac{\left[\frac{\alpha_1\theta_n y}{\cos\frac{\alpha_1\theta_n y}{a}} - \frac{\alpha_1\theta_n y}{\cos\frac{\alpha_1\theta_n y}{a}}\right] e^{-\frac{\theta_n x}{a}}}{\alpha_1^2\sec^2\alpha_1\theta_n - \alpha_2^2\sec^2\alpha_2\theta_n + m(\alpha_1^2-\alpha_2^2)}. \qquad C49$$

Numerical Example

Applying the analysis to panel C shown in Figure 2 with a 1000 compressive load acting on each of the outer flanges, for the given dimensions,

$$P_o = \frac{2000}{2(0.5557)+2(0.5632)+2(0.5618)+0.5612+2(0.099)(2.84)+(0.1014)(2.846)+(0.99)(2.845)}$$

$$= 355.4 \text{ lb.}$$

$$t_x = \frac{2(0.5557)+2(0.5632)+2(0.5618)+0.5612}{2(2.84+2.84+2.845)} = 0.19701 .$$

$$k_x = 1 + \frac{t_x}{t} = 1 + \frac{0.19791}{0.1} = 2.9701 .$$

$$k_y = 1 .$$

$$\frac{1}{k_x k_y} = \frac{1}{2.9701} = 0.3366 .$$

$$\frac{\alpha_1^2}{k_x} = 1 + \mu\left(1 - \frac{1}{k_x k_y}\right) + \sqrt{\left[1 + \mu\left(1 - \frac{1}{k_x k_y}\right)\right]^2 - \frac{1}{k_x k_y}}$$

$$\frac{\alpha_1^2}{k_x} = 1 + \frac{1}{3}(1 - 0.3366) + \sqrt{\left[1 + \frac{1}{3}(1 - 0.3366)\right]^2 - 0.3366}$$

$$= 2.2956.$$

$$\alpha_1 = \sqrt{2.2956(2.9701)} = 2.611$$

$$\frac{\alpha_2^2}{k_x} = 1 + \frac{1}{3}(1-0.3366) - \sqrt{\left[1 + \frac{1}{3}(1-0.3366)\right]^2 - 0.3366} = 0.1466.$$

$$\alpha_2 = \sqrt{0.1466(2.9701)} = 0.6599.$$

θ_n are given by the roots to the equation

$$2.611\tan 2.611\theta - 0.6599\tan 0.6599\theta + m(6.81816 - 0.43542)\theta = 0,$$

where

$$m = \frac{A_F}{ak_x t} = 0.2268,$$

or

$$2.611\tan 2.611\theta - 0.6599\tan 0.6599\theta + 1.4476\theta = 0. \qquad \text{C50}$$

A digital computer program written in Bama Bell for the Univac Solid State 80 computer at the University of Alabama was used to determine the roots to this equation.

It should be noted that the discontinuities existing in Equation C50 can be avoided by rewriting it as

$$2.611\sin 2.611\theta\cos 0.6599\theta - 0.6599\sin 0.6599\theta\cos 2.611\theta$$
$$+ 1.4465\theta\cos 2.611\theta\cos 0.6599\theta = 0. \qquad \text{C51}$$

The computer program used in solving for the roots to Equation C51 is as follows:

```
193     I556901000
194     I506901000
195     I202193223
```

196	0600000000
197	0800000005
198	I201100106
199	5001100400
200	3101400401
201	3102400402
202	R602401403
203	R603401404
204	R602402405
205	R603402406
206	3101406407
207	3407403407
208	3102405408
209	3406408408
210	3103400409
211	3409404409
212	3409406409
213	2407408410
214	1410409410
215	3410104411
216	9411105218
217	R400598000
218	5001410104
219	5001400500
220	1400100400
221	5001250620
222	5001251626

223	R400200000
250	7000010600
251	7000010600
598	5001104299
599	5001400300
600	1500300501
601	3106501501
602	3101501503
603	3102501503
604	R602502504
605	R603502505
606	R602503506
607	R603503507
608	3101507508
609	3508504508
610	3102506509
611	3509505509
612	3103501510
613	3510505510
614	3510507510
615	2508509511
616	1510511510
617	3510299511
618	9511105624
619	5001501300
620	7000010600
621	5001501509

```
622     I241509510
623     R400218000
624     5001501500
625     5001510299
626     7000010600
627     5001501509
628     I241509510
629     R400218000
zzz        193
```

If we write Equation C51 in the general form

$$C_1 \cos C_2\theta \sin C_1\theta - C_2 \cos C_1\theta \sin C_2\theta + C_3\theta \cos C_1\theta \cos C_2\theta = 0, \qquad C52$$

the data used in the computer program and their locations are as follows:

```
100     4850000000
101     C1          (in floating point)
102     C2          (in floating point)
103     C3          (in floating point)
104     5010000000
105     0000000000
106     4950000000
```

The print out format is as follows:

$$\theta \qquad\qquad f(\theta) \ .$$

The magnitude of $f(\theta)$ is an indication of the accuracy of the computation; the nearer it is to zero, the more accurate is the root.

The above program does not have a stop order and will run until the desired number of roots have been found. In this example, the computation was stopped after the first 12 roots were found. They were as follows:

θ	f(θ)
0.9999756	0.40652682
2.1499756	- 0.38730410
2.3500245	- 0.59294616
3.1715868	0.00000013
4.3577845	0.00000570
5.5404765	- 0.00000300
6.6999760	0.27386818
7.1000245	0.38465892
7.9000245	- 0.01819730
9.0980275	- 0.00001230
10.295401	- 0.00002060
11.500111	0.00009496

The above roots to the transcendental equation were used in Equation C48 for the evaluation of the stringer stresses in the x direction. Evaluation of Equation C48 was carried out from x = 0 to x = 24 at increments of x = 1. A digital computer program was also written to perform these calculations. It was as follows:

```
204     I556901000
205     I506901000
206     0600000000
207     0800000005
208     I201098123
209     6700701000
210     3103111400
2111    3112400401
212     R603401401
213     3104401402
```

2141	3112105403
215	R603403403
216	4402403402
217	4401403401
218	3106111404
2191	3112404405
220	R603405405
221	3107405406
2221	3112108407
223	R603407407
224	4406407406
225	4405407405
226	3403403403
227	4099403403
228	3104403403
229	3407407407
230	4099407407
231	3107407407
232	2403407403
233	1403109403
234	R400236000
236	2402406402
237	4402403402
238	R400240000
240	Z082241001
241	5001402599
242	Z100011211

243	R400800000
800	Z092239499
801	Z092241599
8021	3112098415
803	R400244000
244	4415110415
245	R601415415
246	4099415415
2471	R400249000
2491	3600415417
250	1417701701
251	Z100011802
252	3700102700
253	3701101701
254	1100701700
255	R400256000
256	5001098698
257	5001111699
258	I241698700
259	1099098098
260	6700701000
261	7000024802
262	1110111111
263	6098098000
264	7000001209
265	I260000000
266	R403000000
zzz	204

Equation C48 is shown plotted in Figure 7 along with experimental data for comparison.

Stringer Sheet Solution

Consider Fig. C3 which shows a reinforced cylindrical shell. Take axes O_x, O_y, O_z as shown in Fig. C3, O_z being parallel to the axis of the cylinder and O any convenient point of its cross section.

Let w = displacement in direction O_z

s = distance along the circumference, measured from some fixed point on the circumference.

u,v = displacements of the point O parallel to O_x and O_y respectively.

β = angle of rotation of the cross section about O.

Refering to Fig. C3 the displacement of the point P parallel to the tangent at P is

$$\beta h + u\cos\Phi + v\sin\Phi \ . \qquad \text{C53}$$

The shear strain is

$$\varepsilon_{sz} = \frac{\partial w}{\partial s} + \frac{\partial}{\partial z}\left(\beta h + u\cos\Phi + v\sin\Phi\right) \qquad \text{C54}$$

$$= \frac{\partial w}{\partial s} + \frac{\partial}{\partial z}\left(\beta h + u\frac{dx}{ds} + v\frac{dy}{ds}\right)$$

$$= \frac{\partial w}{\partial s} + h\frac{d\beta}{dz} + \frac{du}{dz}\cdot\frac{dx}{ds} + \frac{dv}{dz}\cdot\frac{dy}{ds} = \frac{2(1+\mu)\tau_{sz}}{E}$$

Also, the longitudinal strain

$$\varepsilon_{zz} = \frac{\partial w}{\partial z} = \frac{P_z}{E} \ , \qquad \text{C55}$$

P_z being the average longitudinal stress in skin and stiffeners, as

defined in the first part of this appendix. Summing forces on an element of the shell in direction 0_z,

$$\frac{\partial \tau_{zs}}{\partial z} + k_z \frac{\partial P_z}{\partial z} = 0, \qquad \text{C56}$$

where

$$k_z = 1 + \frac{t_z}{t} . \qquad \text{C57}$$

Substituting Eq. C54 and C55 into Eq. C56,

$$\frac{\partial^2 w}{\partial s^2} + k^2 \frac{\partial^2 w}{\partial z^2} = - \left(\frac{dh}{ds} \cdot \frac{d\beta}{dz} + \frac{du}{dz} \cdot \frac{d^2x}{ds^2} + \frac{dv}{dz} \cdot \frac{d^2y}{ds^2} \right) \qquad \text{C58}$$

where

$$k^2 = 2(1 + \mu)k_z . \qquad \text{C59}$$

For a flat panel, the right hand side of Eq. C58 is zero since the substitutions

$$S = x$$

$$y = 0$$

$$h = 0$$

can be made.

Assuming the fundamental solution

$$w = A[(\cosh\lambda ks)(\cos\lambda z) - 1], \qquad \text{C60}$$

the normal stress is

$$P_z = E \frac{\partial w}{\partial z} = - EA\lambda \cosh\lambda ks(\sin\lambda z) . \qquad \text{C61}$$

The end load in the skin is given by

$$\int_o^a k_z t P_z ds = - \frac{k_z tEA}{k} (\sinh\lambda ka)(\sin\lambda z) \qquad \text{C62}$$

Also, the strain in the flange is equal to the strain in the skin

at z = a. Therefore the end load in one flange is

$$-A_F E A\lambda \cosh\lambda ka(\sin\lambda z) = - mak_z tEA\lambda\cosh\lambda ka(\sin\lambda z) \qquad C63$$

where $A_F = mak_z t$. C64

Integrating from 0 to ∞ with respect to λ to obtain the complete solution,

$$T_o = - \frac{k_z tE}{k} \int_o^\infty A(\sinh\lambda ka + m\lambda ka\cosh\lambda ka)\sin\lambda z d\lambda . \qquad C65$$

Putting $\lambda ka = \theta$, the equation becomes

$$T_o = \frac{k_z tE}{k^2 a} \int_o^\infty A(\theta) \left(\sinh\theta + m\cosh\theta\right) \sin\frac{\theta z}{ka}\, d\theta . \qquad C66$$

If T_o is constant, it may be expressed by the integral

$$T_o = \frac{2T_o}{\pi}\int_o^\infty \sin\frac{\theta z}{ka}\,\frac{d\theta}{\theta} . \qquad C67$$

Equation C66 and C67 are identical, and therefore true for all values of z if

$$A(\theta) = - \frac{2T_o k^2 a}{k_z tE\ (\sinh\theta + m\theta\cosh\theta)} . \qquad C68$$

Hence the required solution, using Eq. C53 is given by

$$w = \int_o^\infty A(\cosh\lambda ks\cos\lambda z - 1)\, d\lambda$$

$$= \frac{2T_o}{\pi k_z tE} \int_o^\infty \frac{1 - \cosh\frac{\theta s}{a}\cos\frac{\theta z}{ka}\ d\theta}{\theta(\sinh\theta + m\theta\cosh\theta)} \qquad C69$$

When evaluated using complex integration, the final result is

$$w = \frac{T_o k}{k_z tE}\left[\frac{z}{ka(1+m)} + 2\sum \frac{\cos\theta_n\ 1 - \cos\frac{\theta_n s}{a}\ e^{-\frac{\theta_n z}{ka}}}{\theta_n(1 + m\cos^2\theta_n)}\right]$$

where the θ_n's are the roots to the equation

$$\tan\theta_n + m\theta_n = 0.$$

Now the normal stress is

$$P_z = P_o\left[1 + 2(1+m)\sum \frac{\cos\theta_n \cdot \cos\frac{\theta_n s}{a}\, e^{-\frac{\theta_n x}{ka}}}{1 + m\cos^2\theta_n}\right] \qquad C70$$

The above Eq. has been written as a function of x to agree with the other solutions in this paper.

Numerical Example

Applying the stringer-sheet analysis to panel B shown in Figure 1 with a 1000 compressive load acting on each of the outer flanges, for the given dimensions

$$P_o = \frac{2000}{0.282 + 0.285 + 0.275 + 0.282 + 0.282 + 0.285 + 0.282 + 0.1(2.61)6}$$

$$= 565.13.$$

$$t_x = \frac{0.282+0.285+0.275+0.282+0.282+0.285+0.282}{6(2.61)} = 0.12598.$$

$$k_x = k_z = 1 + \frac{tx}{t} = 2.2598.$$

$$A_F = 0.282.$$

$$a = 8.69.$$

$$k^2 = 2(1+\mu)k_z$$

$$= 2(1 + \tfrac{1}{3})(2.2598) = 6.026133$$

$$k = 2.455$$

$$m = \frac{A_F}{ak_z t} = \frac{0.282}{0.69(2.2598)(0.1)} = 0.1436.$$

θ_n are the roots to

$$\tan\theta_n + m\theta_n = 0 ,$$

or, rewriting

$$\sin\theta_n + 0.1436\theta_n\cos\theta_n = 0. \qquad C71$$

The computer program used in the determination of the roots to Eq. C51, with some changes, was used in the determination of the roots to the above transcendental equation. Instruction cards 200 through 214 and 602 through 616 were replaced by the following cards:

```
200     R602400401
201     R603400402
202     3161400403
203     3402403402
204     1401402410
205     R602501502
602     R602501502
603     R603501503
604     3101501504
605     3504503503
606     1502250510
607     R400617000
```

If we write Equation C71 in the general form

$$\sin\theta_n + C_1\theta_n\cos\theta_n = 0, \qquad C72$$

the data used in the computer program and their locations are as follows:

100 4850000000

101 C_1 (in floating point)

102 5010000000

103 5010000000

104 5010000000

105 0000000000

106 4950000000

The first 12 roots of Equation C71 were found to be

θ	$f(\theta)$
2.6075298	-0.00000006
5.3973575	-0.00000068
8.3402930	-0.00000053
11.365641	0.00000314
14.433643	-0.00000176
17.525235	0.00000531
12.630902	-0.00000340
23.745538	0.00000264
26.866203	-0.00000151
29.991100	0.00000269
33.119075	-0.00000353
36.249355	0.00000697

The above roots to the transcendental equation were used in Equation C70 for the evaluation of the stringer stresses in the x direction. Evaluation of Equation C70 was carried out from x = 0 to x = 24 at increments of x = 1. A digital computer program was written to perform these calculations. It was as follows:

193 I556901000

194	I506901000
195	I202193226
196	R400197000
197	0600000000
198	0800000005
199	I201099116
200	6700702000
2011	R603105400
202	3400400400
203	3103400401
204	1101401401
205	4400401401
206	Z082207001
207	5001401599
208	Z010011201
209	Z092207599
2101	Z105099410
211	4410104410
212	R601410410
213	4101410410
2141	3500410415
215	1415702702
216	Z100011210
217	3702102702
218	1101702702
219	3702100702
220	5001099701

```
221     I241701702
222     1101099099
223     6700702000
224     7000023210
225     I260000000
226     R403000000
zzz        193
```

Equation C70 is shown plotted in Figure 8 along with experimental data for comparison.

APPENDIX D

THE SUBSTITUTE SINGLE STRINGER METHOD

In this appendix, the substitute-single-stringer method presented by Kuhn and Chiarito in Reference 19 will be applied to panel C.

The analysis of a multistringer panel by the substitute single stringer method requires the following steps:

1. The properties of the substitute panel are established as follows:
   A. The substitute single stringer is first located at the centroid of the internal forces in the stringers. Although the sheet is assumed to carry only shear stresses, an effective width of sheet is considered to be acting with the sheet. The distance from the outer flange to the centroid of the stringer areas is b_c.
   B. The area of the flange in the substitute panel is equal to the area of the flange in the actual panel. The area of the substitute stringer is equal to the sum of the areas of the stringers in the actual panel plus the effective area of sheet acting with them.
   C. The substitute stringer is then located according to the empirical relation

$$b_s = \left[0.65 + \frac{0.35}{n^2}\right] b_c$$

   where n is the number of stringers in the half panel.

2. The substitute panel is analyzed as follows:

   From Fig. D1-b

$$A_F\sigma_F + \tau t dx - (\sigma_F + d\sigma_F)A_F = 0$$

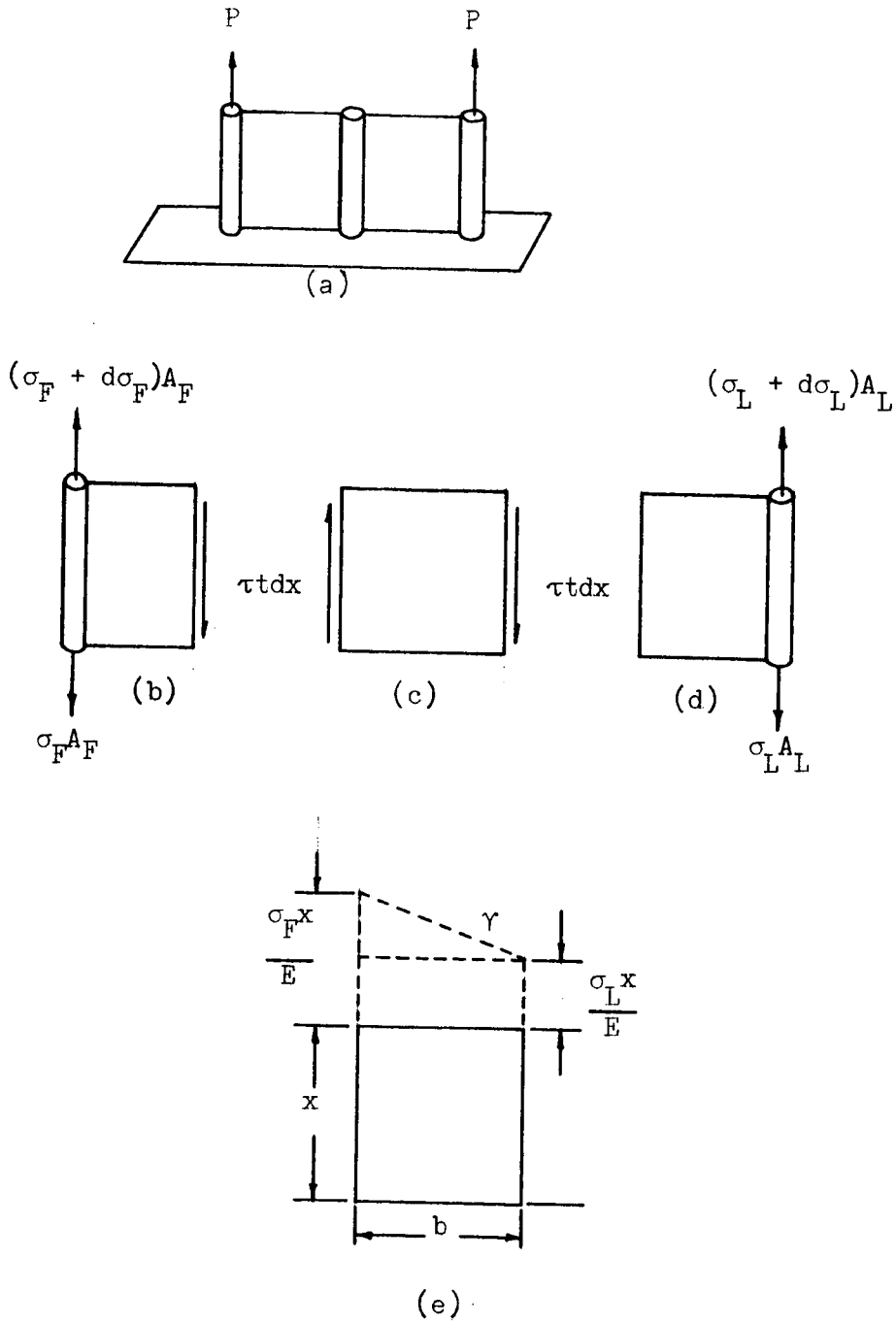

Figure D1--Three stringer panel with symmetrical axial load.

$$A_F d\sigma_F = \tau t dx \ .$$

Also,

$$A_L(\sigma_L + d\sigma_L) - A_L\sigma_L + \tau t dx = 0$$

$$A_L d\sigma_L = -\tau t dx$$

so

$$A_F d\sigma_F = \tau t dx = -A_L d\sigma_L \ . \qquad \text{D1}$$

From Fig. D1-e, the shear strain at station x is given by

$$\gamma = \frac{x}{bE}(\sigma_F - \sigma_L) \ .$$

The increment of shear strain is

$$d\gamma = \frac{(\sigma_F - \sigma_L)}{bE} dx \ .$$

The increment of shear stress is

$$d\tau = G d\gamma = \frac{G}{bE}(\sigma_F - \sigma_L)dx \ . \qquad \text{D2}$$

Differentiating Eq. D2,

$$\frac{d^2\tau}{dx^2} = \frac{G}{bE}(d\sigma_F - d\sigma_L) \ . \qquad \text{D3}$$

Substituting Eq. D1 into Eq. D3,

$$\frac{d^2\tau}{dx^2} = \frac{G}{bE}\left[\frac{\tau t}{A_F} + \frac{\tau t}{A_L}\right] ,$$

or

$$\frac{d^2\tau}{dx^2} - k^2\tau = 0, \qquad \text{D4}$$

where

$$k = \sqrt{\frac{Gt}{bE}\left[\frac{1}{A_F} + \frac{1}{A_L}\right]} \ . \qquad \text{D5}$$

Assuming a solution to Eq. D4 of the form

$$\tau = C_1 e^{kx} + C_2 e^{-kx}, \qquad \text{D6}$$

application of the boundary condition $\tau = 0$ at $x = 0$ yields

$$0 = C_1 e^{0} + C_2 e^{-0}.$$

$$\therefore C_1 = -C_2 ,$$

so

$$\tau = C_1 (e^{kx} - e^{-kx}). \qquad \text{D7}$$

Differentiating Eq. D7

$$\frac{d\tau}{dx} = C_1 k (e^{kx} + e^{-kx}) .$$

Equating equations D2 and D8,

$$C_1 = \frac{G(\sigma_F - \sigma_L)}{bEk(e^{kx} + e^{-kx})} . \qquad \text{D9}$$

Application of the boundary condition $\sigma_F = P/A_F$, $\sigma_L = 0$ at $x = L$ yields

$$C_1 = \frac{G(P/A_F)}{bEk(e^{kL} + e^{-kL})} . \qquad \text{D10}$$

Substituting Eq. D10 into Eq. D7,

$$\tau = \frac{GP}{bEA_F k} \frac{\sinh kx}{\cosh kL} . \qquad \text{D11}$$

Defining

$$A_T = A_F + A_L$$

and substituing into Eq. D5,

$$k = \frac{GtA_T}{bEA_F A_L} . \qquad \text{D13}$$

Now, from Eq. D11,

$$\tau = \frac{GPk}{bEA_F k^2} \frac{\sinh kx}{\cosh kL} = \frac{GPk}{bEA_F \left(\frac{GtA_T}{bEA_F A_L} \right)} \frac{\sinh kx}{\cosh kL} ,$$

$$\tau = \frac{PkA_L}{tA_T} \frac{\sinh kx}{\cosh kL} . \qquad \text{D14}$$

Substituting Eq. D14 into Eq. D1

$$d\sigma_F = \frac{t}{A_F} \tau dx = \frac{PkA_L}{A_F A_T} \frac{\sinh kx}{\cosh kL} dx . \qquad \text{D15}$$

Integrating,

$$\sigma_F = \frac{PA_L}{A_F A_T} \frac{\cosh kx}{\cosh kL} + C_3 . \qquad \text{D16}$$

Since $\sigma_F = P/A_F$ at $x = L$,

$$\frac{P}{A_F} = \frac{PA_L}{A_F A_T} + C_3 .$$

$$\therefore C_3 = \frac{P}{A_F} \left[1 - \frac{A_L}{A_T} \right] = \frac{P}{A_F} \left[\frac{A_T - A_L}{A_T} \right] = \frac{P}{A_F} \left[\frac{A_F + A_L - A_L}{A_T} \right] = \frac{P}{A_T} . \qquad \text{D17}$$

Now

$$\sigma_F = \frac{PA_L}{A_F A_T} \frac{\cosh kx}{\cosh kL} + \frac{P}{A_T} = \left[1 + \frac{A_L}{A_F} \frac{\cosh kx}{\cosh kL} \right] \frac{P}{A_T} . \qquad \text{D18}$$

Also from Eq. D1

$$d\sigma_L = - \frac{t}{A_L} \tau dx = - \frac{Pk}{A_T} \frac{\sinh kx}{\cosh kL} dx . \qquad \text{D19}$$

Integrating,

$$\sigma_L = - \frac{P}{A_T} \frac{\cosh kx}{\cosh kL} + C_4 . \qquad \text{D20}$$

Since $\sigma_L = 0$ at $x = L$,

$$C_4 = \frac{P}{A_T} .$$

$$\therefore \sigma_L = \frac{P}{A_T}\left[1 - \frac{\cosh kx}{\cosh kL}\right]. \qquad D21$$

Equations D14, D18, and D21 determine the stress distribution in the substitute stringer. Taking the origin at the tip, the change in coordinates can be expressed as

$$x = L - x_1 . \qquad D22$$

Now the approximation

$$\frac{\sinh kx}{\cosh kL} = \frac{\sinh k(L-x_1)}{\cosh kL} = \frac{\sinh kL \cosh kx_1}{\cosh kL} - \frac{\cosh kL \sinh kx_1}{\cosh kL}$$

$$= \tanh kL \cosh kx_1 = \frac{1}{2}(e^{kx_1}+e^{-kx_1}-e^{kx_1}+e^{-kx_1}) = e^{-kx_1} \qquad D23$$

may be made, since $\tanh kL \to 1$ for large values of kL.

Dropping the subscript on the x and considering the tip as the origin, Equations D14, D18, and D21 may now be written

$$\tau = \frac{PkA_L}{tA_T} e^{-kx}, \qquad D24$$

$$\sigma_F = \frac{P}{A_T}\left[1 + \frac{A_L}{A_F} e^{-kx}\right] , \qquad D25$$

$$\sigma_L = \frac{P}{A_T}(1 - e^{-kx}) . \qquad D26$$

Numerical Example

For panel C, the location of the centroid of the internal forces is (using an effective width equal to one half the distance between stringers)

$$b_c = \frac{1}{3(2.5575)+3(0.565)+0.280}\,[(2.5575+4.265+7.11)(2.275)(0.1)$$

$$+2.84(0.564)(1)+5.69(1)+8.1075(0.280)(1)] ,$$

$$b_c = 3.740.$$

The areas of the substitute stringer and the flange are

$$A_L = 0.7917 + 0.7908 + 0.3938 = 1.9763 \text{ in}^2.$$

$$A_F = 0.565 \text{ in}^2.$$

The location of the substitute stringer is

$$b_s = (0.65 + 0.35/2^2)(3.740) = 2.75825 \text{ in.}$$

Now substituting the above into the appropriate formulas

$$k = \sqrt{\frac{(3.9)(10^6)(0.1)}{(10.5)(10^6)(2.75825)}\left[\frac{1}{0.565} + \frac{1}{1.9763}\right]} = 0.17503 .$$

$$A_T = A_F + A_L = 0.565 + 1.9763 = 2.5413 \text{ in}^2.$$

$$\tau = \frac{PkA_L}{tA_T} e^{-kx} = \frac{1000(0.17503)(1.9763)}{0.1(2.5413)} e^{-0.17503x}$$

$$= 1,361.15e^{-0.17503x}.$$

$$\sigma_F = \frac{P}{A_T}\left[1 + \frac{A_L}{A_F} e^{-kx}\right] = \frac{1000}{2.5413}\left[1 + \frac{1.9763}{0.565} e^{-0.17503x}\right]$$

$$= 393.5 + 1,376.4e^{-0.17503x}.$$

$$\sigma_L = \frac{P}{A_T}\left[1 - e^{-kx}\right] = \frac{1000}{2.5413}(1 - e^{-0.17503x})$$

$$= 393.5(1 - e^{-0.17503x}).$$

The above equations are shown plotted in Figure 11 with experimental data for comparison.

APPENDIX E

MINIMUM ENERGY SOLUTION USING MATRIX METHODS

Dividing panel C into bays with generalized forces as shown in Figure E1, results in a statically indeterminate system which may be solved by matrix methods. The type of stress distribution assumed as well as the number of bays used determine the accuracy of the method. For this analysis it was assumed that the stiffeners transmit only normal stresses and the sheet material transmits only shearing stresses. It was further assumed that the panel and loading are symmetrical.

The notation used is the same as used by Bruhn [4].

For the analysis the following matrix operations are required:

1. Evaluate $\left[a_{rn}\right] = \left[g_{ri}\right]\left[a_{ij}\right]\left[g_{jn}\right]$

2. Evaluate $\left[a_{rs}\right] = \left[g_{ri}\right]\left[a_{ij}\right]\left[g_{js}\right]$

3. Evaluate $\left[a_{rs}^{-1}\right]$ the inverse of $\left[a_{rs}\right]$

4. Evaluate $\left[G_{rm}\right] = \left[a_{rs}^{-1}\right]\left[a_{rn}\right]$

5. Evaluate $\left[G_{im}\right] = \left[g_{im}\right] + \left[g_{ir}\right]\left[G_{rm}\right]$

6. Evaluate $\left[q_{in}\right] = \left[G_{im}\right]\left[P_{mn}\right]$

7. As a check the matrix

$$\left[A_{rn}\right] = \left[g_{ri}\right]\left[a_{ij}\right]\left[G_{jn}\right]$$

may be evaluated. If all matrix operations have been exact, each element of $\left[A_{rn}\right]$ should be zero. Due to rounding errors some of the elements may not be zero, but they should be small compared with corresponding elements of $\left[a_{rn}\right]$.

A Fortran IV program was written to perform the above matrix operations and the computation for panels B and C was performed by the Univac 1107 at the University of Alabama Research Institute located in Huntsville, Alabama.

Results of these analyses are shown compared with experimental data in Figures 12 and 13.

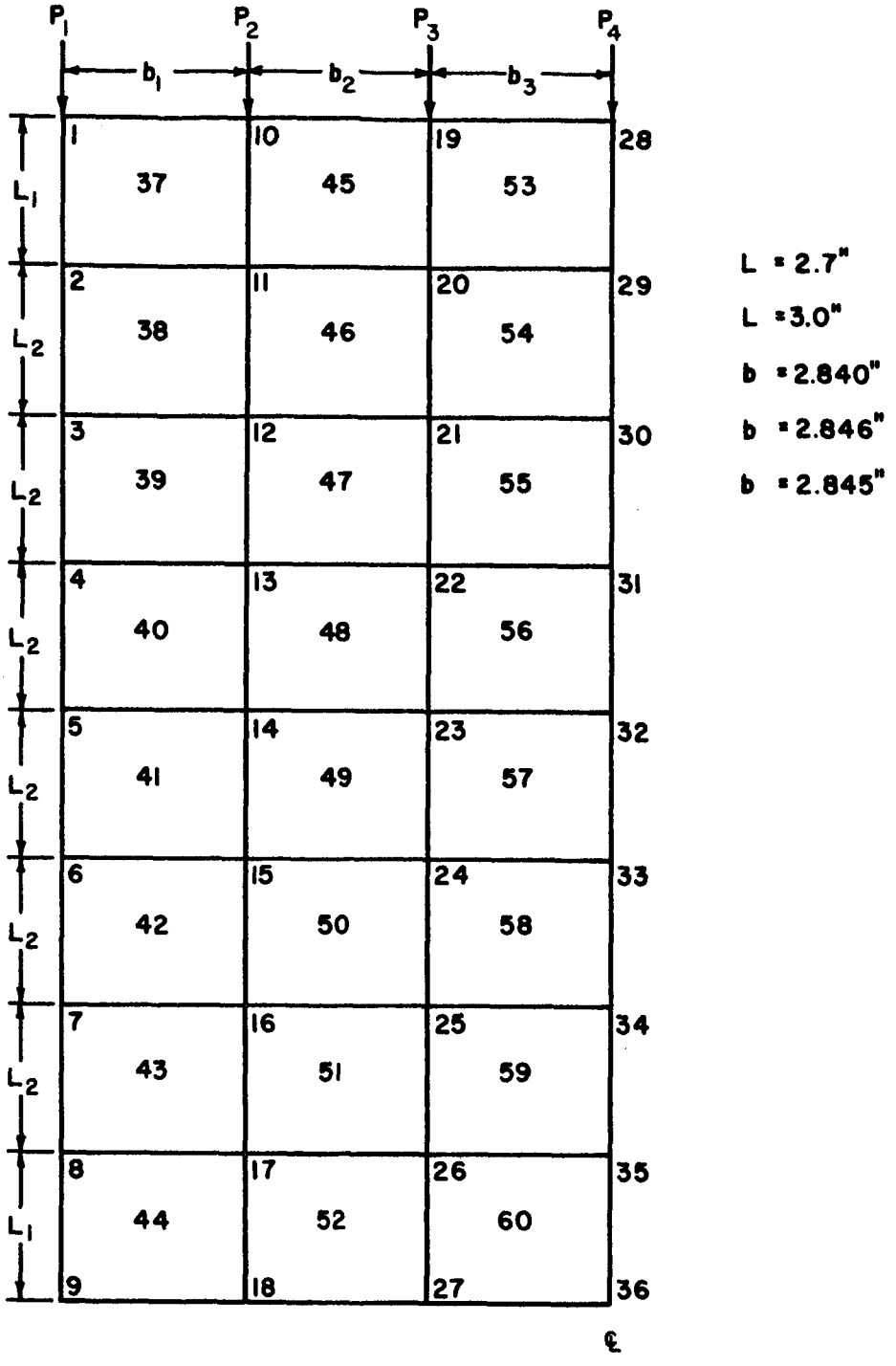

FIGURE E1 GENERALIZED FORCE SYSTEM USED IN MATRIX ANALYSIS OF PANEL C. THE PANEL AND LOADING ARE ASSUMED TO BE SYMMETRICAL.

REFERENCES

1. Akao, S.: Analysis of Shear Lag Problems by Means of Difference Equations. Technol. Rep. Osaka Univ., Vol. 9, March 1959, pp. 91-99.

2. Anderson, R. A. and Houbolt, J. C.: Effect of Shear Lag on Bending Vibration of Box Beams. NACA TN 1583, 1948.

3. Borsari, P. and Yu, A.: Shear Lag in a Plywood Sheet Stringer Combination Used for the Chord Member of a Box Beam. NACA TN 1443, 1948.

4. Bruhn, Elmer F.: Analysis and Design of Flight Vehicle Structures. Tri State Offset Company, Cincinnati, Ohio, 1965.

5. Chiarito, P. T.: Shear Lag Tests of Two Box Beams with Corrugated Covers Loaded to Failure. NACA Wartime Rep. L-482, 1944.

6. Chiarito, P. T.: Shear Lag Tests of Two Box Beams with Flat Covers Loaded to Destruction. NACA Wartime Report L-307, 1942.

7. Cox, H. L.: Stress Analysis of Thin Metal Construction. Journal of the Royal Aeronautical Society, Vol. 44, March, 1940, pp. 231-282.

8. Davenport, W. W. and Kruszewski, E. T.: A Substitute-Stringer Approach for Including Shear-Lag Effects in Box Beam Vibrations. NACA TN 3158, 1954.

9. Duncan, W. J.: Diffusion of Load in Certain Sheet-Stringer Combinations. ARC (Great Britain), R. and M. No. 1825, 1938.

10. Fine, M.: A Comparison Between Plain and Stringer Reinforced Sheet from the Shear Lag Standpoint. ARC (Great Britain), R. and M. No. 2618, 1942.

11. Gantmacher, F. R.: The Theory of Matrices, Vol. 1. Chelsea Publishing Company, New York, New York, 1960.

12. Goland, M.: Shear Lag Solutions for Sheet-Stringer Panels by Means of a Hydrodynamic Analogy. Journal of the Aerospace Sciences, Vol. 27, April 1960, pp. 291-295, 303.

13. Goodey, W. J.: Stress Diffusion Problems. Aircraft Engineering, Vol. 18, 1946, pp. 227-230, 234, 271-276, 313-316, 343-346, 385-389.

14. Kempner, J.: Recurrence Formulas and Differential Equations for Stress Analysis of Cambered Box Beams. NACA TN 1466, 1947.

15. Kuhn, P.: Approximate Stress Analysis of Multi-Stringer Beams with Shear Deformation of the Flanges. NACA Rep. No. 636.

16. Kuhn, P.: Stress Analysis of Beams with Shear Deformation of the Flanges. NACA Report No. 608.

17. Kuhn, P.: Shear Lag Stresses in Aircraft and Shell Structures. McGraw-Hill Book Company, Inc., 1956, pp. 101-154, 354-382.

18. Kuhn, P.: A Recurrence Formula for Shear Lag Problems. NACA TN 739, 1939.

19. Kuhn, P. and Chiarito, P.: Shear Lag in Box Beams--Methods of Analysis and Experimental Investigations. NACA TR 739, 1943.

20. Kuhn, P. and Peterson, J. P.: Shear Lag in Axially Loaded Panels. NACA TN 1728, 1948.

21. Lovett, B. B. C. and Rodee, W. F.: Transfer of Stress from Main Beams to Intermediate Stiffeners in Metal Sheet Covered Box Beams. Journal of the Aeronautical Sciences, Vol. 3, October 1936, pp. 426-430.

22. Lundquist, E. E.: Comparison of Three Methods for Calculating the Compressive Strength of Flat and Slightly Curved Sheet and Stringer Combinations. NACA TN 455.

23. Newton, R. E.: Electrical Analogy for Shear Lag Problems. Proceedings of the Society for Experimental Stress Analysis, Vol. 2, No. 2, 1945, pp. 71-80.

24. Peterson, J. P.: Shear Lag Tests on a Box Beam with a Highly Cambered Cover in Tension. NACA Wartime Report L-106, 1945.

25. Reissner, E.: On the Problem of Stress Distribution in Wide Flanged Box Beams. Journal of the Aeronautical Sciences, Vol. 5, June 1938, pp. 295-299.

26. Rey, William K.: A Study of the Stability of Reinforced Cylindrical and Conical Shells Subjected to Various Types and Combinations of Loads, Section IV--Matrix Shear Lag Analysis Utilizing a High Speed Digital Computer. Bureau of Engineering Research, University of Alabama, November 1962 .

27. Ross, R. D.: An Electrical Computer for the Solution of Shear-Lag and Bolted Joint Problems. NACA TN 1281, May 1947.

28. White, R. J. and Antz, H. M.: The Stress Distribution in Reinforced Plates Under Concentrated Edge Loads. Journal of Aeronautical Sciences, Vol. 3, No. 6, April 1936, pp. 209-212.

29. Winny, H. F.: The Distribution of Stress in Monocoque Wings. ARC (Great Britain), R. and M. No. 1756, 1938.

30. Younger, J. E.: Miscellaneous Collected Airplane Structural Design Data, Formulas, and Methods. A.C.I.C. No. 644, Materiel Division, Army Air Corps, 1930.